Magnetic fluctuations in the classical *XY* model: The origin of an exponential tail in a complex system

S. T. Bramwell,[1] J.-Y. Fortin,[2,*] P. C. W. Holdsworth,[3,†] S. Peysson,[3] J.-F. Pinton,[3] B. Portelli,[3] and M. Sellitto[3]
[1]*Department of Chemistry, University College London, 20 Gordon Street, WC1H OAJ London, United Kingdom*
[2]*Department of Physics, University of Washington, Seattle, Washington 98195*
[3]*Laboratoire de Physique, Ecole Normale Supérieure de Lyon, 46 Allée d'Italie, F-69364 Lyon Cedex 07, France*
(Received 8 August 2000; published 21 March 2001)

We study the probability density function for the fluctuations of the magnetic order parameter in the low-temperature phase of the *XY* model of finite size. In two dimensions, this system is critical over the whole of the low-temperature phase. It is shown analytically and without recourse to the scaling hypothesis that, in this case, the distribution is non-Gaussian and of universal form, independent of both system size and critical exponent η. An exact expression for the generating function of the distribution is obtained, which is transformed and compared with numerical data from high-resolution molecular dynamics and Monte Carlo simulations. The asymptotes of the distribution are calculated and found to be of exponential and double exponential form. The calculated distribution is fitted to three standard functions: a generalization of Gumbel's first asymptote distribution from the theory of extremal statistics, a generalized log-normal distribution, and a χ^2 distribution. The calculation is extended to general dimension and an exponential tail is found in all dimensions less than 4, despite the fact that critical fluctuations are limited to $D=2$. These results are discussed in the light of similar behavior observed in models of interface growth and for dissipative systems driven into a nonequilibrium steady state.

DOI: 10.1103/PhysRevE.63.041106 PACS number(s): 05.40.−a, 05.50.+q, 75.10.Hk

I. INTRODUCTION

A. Motivation for the present work

The fluctuations in a global measure of a many-body system are often assumed to be of Gaussian form about the mean value [1]. This assumption is nearly always true if the system in question can be divided into statistically independent microscopic or mesoscopic elements [2], as dictated by the central-limit theorem (see Appendix A). However, in correlated systems, where this is not the case, there is no universal reason to expect the central-limit theorem to apply. The spectrum of fluctuations can then take on a multitude of different mathematical forms, including those of other, well-defined, limit distributions.

In this context, the most studied correlated systems are critical systems. At the critical point of a second-order phase transition, a correlation length, ξ, diverges from the microscopic scale (taken as unity throughout the paper). It is only cut off, in an ideal world, by the macroscopic or integral scale L. The probability density function (PDF) for the order parameter m associated with the diverging correlation length is essentially the exponential of the free energy $P(m) \sim \exp(-F(m)/k_BT)$ and takes on an approximately Gaussian form as long as the Landau approximation, $F(m) \sim a + bm^2 + \cdots$, is valid. Close to the critical point, the Landau approximation breaks down and the PDF becomes non-Gaussian. The key assumption of the renormalization-group theory of critical phenomena is that the critical PDF remains scale invariant in the thermodynamic limit and can be obtained from the fixed point of a renormalization-group transformation [3,4] (see Appendix A). Thus, renormalization-group theory can be regarded as a generalization of the central-limit theorem to systems that are correlated over all length scales. The critical PDFs can be termed ''universal,'' in that, when properly normalized, they depend on at most a few basic symmetries that define the universality class of the system. A non-Gaussian and universal PDF is therefore a direct signature of the fluctuation-driven critical phenomena that have revolutionized modern statistical mechanics [5]. Analytical and numerical work [6–9] on Ising, Potts, and *XY* models has shown that a generic feature of such systems is a skewness, with large fluctuations below the mean, towards small order-parameter values.

Correlations that are both strong and long range are a feature not only of critical phenomena but also of systems driven far from equilibrium. However, in the case of driven systems, the absence of a microscopic theory means that one has to rely heavily on empirical observations from experiment and numerical simulation. Labbé *et al.* [10] have shown that the PDF for the energy injected into a closed turbulent flow at constant Reynolds number is also non-Gaussian and universal. In this case, ''universal'' means that the PDF, when suitably normalized, does not depend on the Reynolds number or several other parameters (for example, the type of fluid). The PDF again has a marked skewness with an apparent exponential tail for fluctuations towards low energies.

The present work is motivated by our empirical observation [11,12] that the universal PDF of energy fluctuations in the turbulence experiment [10,13] is, within experimental error, of the same functional form as that of the universal

*Permanent address: CNRS, UMR 7085, Laboratoire de Physique Théorique, Université Louis Pasteur, 67084 Strasbourg, France.
†Author to whom correspondence should be addressed. Electronic address: peter.holdsworth@ens-lyon.fr

$P(m)$ for the critical system that we have studied. The latter is the spin-wave limit to the low-temperature phase of the two-dimensional) (2D) XY model [14,15] that is known to capture the critical behavior of the full 2D XY model [16–20]. The distribution is shown in Fig. 2: it is asymmetric, with fluctuations below the mean approaching an exponential asymptote, while those above the mean approach a double exponential. This observation led us to the proposition that many systems, both equilibrium and nonequilibrium, sharing the property of long-range correlations and multiscale fluctuations, should share the same features, at least to a good approximation [11,21]. The proposition appears to be strikingly confirmed in Ref. [21], where, from numerical simulation, similar behavior is observed in a number of different systems: for order-parameter fluctuations in the two-dimensional Ising model and in the two-dimensional percolation problem, as well as for fluctuations in global quantities for models of forest fires and avalanches, driven into a self-organized critical state. This appears to contradict the idea that the PDF should depend on the particular universality class of the model in hand. One possible way of accounting for our observations is that many universality classes share common features, with the differences between them appearing either outside the range of physical observation, or being hidden by experimental error. There are therefore many open questions regarding a possible and much desired connection between critical phenomena and nonequilibrium systems as well as regarding the details of the PDF in critical systems. It is these questions that we address in the current paper, via an analytic study of the PDF for order-parameter fluctuations in a finite XY model in arbitrary dimension.

B. Normalization of the order parameter

We discuss order-parameter fluctuations of finite systems in terms of distributions that are calculated in the thermodynamic limit, $N\rightarrow\infty$. As discussed in Appendix A, it is essential to normalize the order parameter by an appropriate power of $N=L^D$ in order to obtain a distribution of finite width, or, equivalently, a form for $P(m)$ that is independent of system size. By extending the scaling hypothesis to include finite systems [22], the following form of $P(m)$ has been proposed:

$$P(m,L)\sim L^{\beta/\nu}P_L(mL^{\beta/\nu},\xi/L). \tag{1}$$

Here β and ν are the conventionally defined critical exponents for the magnetization and correlation length ξ, respectively [22]. The appropriate normalization of the order parameter is provided by the factor $L^{-\beta/\nu}$ while fixing different ratios ξ/L will in principle result in an infinity of different limit distributions as $L\rightarrow\infty$. We concentrate on the case of a truly critical system with correlations over all length scales, which should result in maximum deviation from the Gaussian form. Here the dependence on ξ can be dropped from Eq. (1), and $P_L(m)$ should closely approximate a single universal function of the variable $mL^{\beta/\nu}$ for all values of L. In this form it is independent of the microscopic details of the system, although it could indeed depend on the universality class of the transition through the critical exponents.

Equation (1) is demystified somewhat by recognizing that the normalizing factor $L^{-\beta/\nu}$ is, in such an ideal system, proportional to the mean value of the order parameter, $\langle m\rangle$. Further, one of the key properties of a critical system is that the standard deviation of the distribution, σ, scales with system size in the same way as the mean value. This property, which is a direct result of the hyperscaling relation and that we refer to as the hyperscaling condition, means that Eq. (1) can alternatively be written in the form $P(m)=1/\sigma P_L(m/\sigma)$. Thus σ provides, as might be intuitively expected, the correct normalization of the order parameter, such that a reasonable PDF of finite width is obtained in the limit $N\rightarrow\infty$. In this paper, in addition, we shift the distribution with respect to the mean value and define

$$\sigma P(m)=\Pi(\theta), \tag{2}$$

where

$$\theta=\frac{m-\langle m\rangle}{\sigma}. \tag{3}$$

In this representation one expects the PDF to fall, in the thermodynamic limit, onto a single universal curve. Provided that finite-size corrections to scaling are negligible, one should observe data collapse onto this universal curve for large but finite system sizes.

C. The two-dimensional XY model

The model that we study, the harmonic spin-wave limit to the XY model, is defined in Sec. II for the case of two dimensions, $D=2$. This is the dimension of most interest in the present context, as the system is at its lower critical dimension. At low temperature, the coupling J/k_BT is an exactly marginal variable that characterizes a line of critical points in zero applied field [23]. The critical line is separated from the paramagnetic phase by the Kosterlitz-Thouless-Berezinskii phase transition at T_{KTB} [16,17]. The critical phase that exists below this temperature is an attractive subject of investigation from both an analytic and a numerical point of view. Its physics is entirely captured by the harmonic Hamiltonian [16,19,20] with the result that many calculations can be performed microscopically, without the need to use renormalization techniques, or the scaling hypothesis. From a numerical point of view, simulation results near a single, isolated, critical point are often complicated by a shift in the effective critical temperature by an amount scaling to zero as $L^{-1/\nu}$ [7–9], making it unclear exactly which temperature should be studied. Indeed, numerical studies of Ising and Potts models [7–9] do find distributions whose form depends on temperature in the critical region (see Appendix A). In the 2D XY model, as the system is critical over a range of temperatures there are no such technical problems and data for $P(m)$ can be collected at all points below T_{KTB}. These factors make the 2D XY model an ideal system with which to study the effects of critical correlations.

The finite-size scaling for the 2D XY model has been discussed in our previous publications [14,15]. In this work, we began, following Berezinskii [16] and Rácz and Plischke

[24], an exact calculation for the PDF of order-parameter fluctuations. This calculation is completed and presented in detail in the current paper (Sec. II). It shows explicitly that the non-Gaussian behavior in the 2D XY model stems from the influence of all length scales from the microscopic to the macroscopic scale. We propose that the same is true for other complex systems including those driven far from equilibrium. This provides a basis for understanding the apparent overlap of their PDFs and provides an unexpected experimental motivation for studying a system as simple as the 2D XY model.

Two results coming out of our calculation are worthy of note at this stage. The first is an exact analytic result that is rather surprising given the previous discussion and the general belief concerning the dependence of the PDF on universality class: shifting the curve with respect to the mean, Eq. (2), gives us universal data collapse, not only for all system size but also for all temperatures for which the harmonic Hamiltonian is valid. The ratio of exponents β/ν depends linearly on temperature, from which we deduce that the PDF is independent of the value of the exponents along the line of critical points. One should note, however, that these points are rather special and the result cannot necessarily be generalized to all critical points: not all the usual critical exponents are defined. For example, the exponents β and ν are not individually defined, but their ratio is [17]. The usual scaling relations are valid in terms of the ratio β/ν only and this ''weak scaling'' [18] means that there is only one independent critical exponent, $\eta=2\beta/\nu$ [17], compared with two for a regular critical point. This is all that is required for the analysis leading to Eq. (1), but is not sufficient to ensure a unique functional form for the general problem with two exponents. However, it does seem consistent with the idea that only small differences separate results for different universality classes.

The second result, which is relevant to mention at this stage, concerns the finite-size scaling data collapse of Eq. (2). We find that the hyperscaling property $\sigma\sim\langle m\rangle$ is not a necessary condition for data collapse onto a non-Gaussian function. With our definition (2), the first two moments of $P(m)$ fall trivially out of the calculation and all that is required for data collapse is that the moments $\langle\theta^p\rangle$ for $p>2$ are independent of the system size. This is the most general condition for non-Gaussian data collapse, while the PDF only satisfies the scaling hypothesis in the form of Eq. (1), if the hyperscaling condition is satisfied. We give, in Sec. II A, an explicit example where data collapse onto the universal curve of the 2D XY model occurs, but where the hyperscaling condition is not satisfied. If we make an expansion of the order parameter about a perfectly ordered state ($m=1$) in powers of temperature, keeping only the linear term, then $\langle m\rangle$ diverges logarithmically with system size [25,26], while the standard deviation is a constant. The ratio $\sigma/\langle m\rangle$ is actually an *increasing* function of system size throughout the physical domain. It is only when the order parameter is correctly defined on the interval [0,1] that the hyperscaling relation is reestablished, but written in the form (2) the two distinct variables have the same universal PDF, even outside the range of temperature and system size for which the development gives an accurate representation of the true order parameter. This result is more than a mathematical curiosity; the harmonic approximation for the 2D XY model maps directly onto the Edwards-Wilkinson (EW) model [27–29,31] for interface growth and the linearized order parameter is related to the square of the interface width, w: $m=1-w^2$. Our PDF, therefore, corresponds precisely to that for interface width fluctuations and for which, in two dimensions, the hyperscaling condition for the observable w^2 is explicitly violated.

D. Organization of the paper

The rest of the paper is organized as follows. In Sec. II, we present details of the calculation for the PDF in the 2D XY model. (For convenience, throughout this paper we use the term ''XY model'' to refer to either the model defined by the spin-wave Hamiltonian or the full XY model over a temperature range in which the spin-wave approximation is valid. This should not cause any confusion in reading the present paper, but our choice of terminology should be borne in mind when comparing to other work on the XY model.) We show explicitly that it is a universal function of system size and of temperature and find an exact expression for the characteristic function (Sec. II A). Transforming the distribution numerically, we compare it in detail with extensive Monte Carlo and molecular-dynamics simulations of the full XY model and show that it is clearly the complete solution of the problem (Sec. II B). We calculate the asymptotic values of the distribution for large deviations below and above the mean, which we find to be exponential and double exponential, respectively (Secs. II C and II D).

In Sec. III, we try to fit the computed PDF to standard functions by comparing the moment expansion of the generating function with those of the Fourier transform of the test function. Three functions are considered:

$$\Pi(\theta)\sim\begin{cases}\exp a[\theta-s-\exp(\theta-s)],\\ \dfrac{1}{s-\theta}\exp\{-[\ln(s-\theta)-a]^2\},\\ (s-\theta)^{\nu/2-1}e^{-a(s-\theta)}.\end{cases}\tag{4}$$

The PDF is fitted to an excellent approximation over the physical range by the first two functions, while the third gives a reasonable but slightly inferior fit. The first function, with a an integer, comes from extremal statistics (Sec. III A). It is Gumbel's first asymptote, corresponding to the PDF for the ath largest value from ensembles of N random numbers [32]. The interpretation with a noninteger (we find $a=\pi/2$) is not clear, but a connection between critical phenomena and extremal statistics is a very appealing concept [33,34]. The second function is a generalized log-normal distribution (Sec. III B). Unlike the first curve, it does not have the correct asymptotic forms but despite this it fits just as well over the physical domain. The third function is a χ^2 distribution describing identical and statistically independent degrees of freedom (Sec. III C). It gives reasonable qualitative agree-

ment indicating that a good, zeroth-order description of a correlated system is in terms of a reduced number of statistically independent variables. However, this description has its limits, as shown by the fact that this function fits the exact PDF slightly less well than the other two. This variety of different fits suggests that one should treat the physical interpretations that they offer with caution; however, even with this caveat in mind they still represent useful mathematical tools. To investigate this point further, in Sec. III D we derive an approximate functional form for the curve using an analysis due to Pearson that reconstructs the PDF from the four principal moments, which in this case have been calculated analytically. The Pearson analysis gives a quite different function, which also gives a good description of the exact PDF over a physical range of θ. This serves to emphasize that, given zero mean and unit variance, the shape of the curve over a typical experimental range is essentially defined by its skewness, γ, and kurtosis, κ. Therefore, an alternative way of summarizing the observed universality [11,21] is that γ and κ, for several different systems, have the same scale-invariant values as they do for the XY model.

In Sec. IV, we extend our calculation to D dimensions, which apart from $D=2$ are all noncritical. Despite this, we find evidence of the integral scale for all dimensions $D<4$. For $D=1$, the PDF for the linearized order parameter shows an exponential tail. However, we show numerically that the PDF for the correctly defined order parameter is quite different and is just what one would expect for a paramagnetic system without correlations (Sec. IV A). The case $D=3$ holds a final surprise (Sec. IV B): despite the long-range order of the low-temperature phase, the PDF is still not a Gaussian function. The temperature is a dangerously irrelevant variable in the ordered phase of the 3D XY model with the result that the susceptibility remains weakly divergent at low temperature [35]. The result of this divergence is that the asymptotes of the PDF for large fluctuations are exponential below the mean and $\exp(-\mathrm{cst}\,\theta^3)$ above the mean (where ''cst'' is a constant). The hyperscaling relation, in this case, is again violated. The divergence disappears at the upper critical dimension and we find a truly Gaussian PDF for $D \geqslant 4$.

In Sec. V, we conclude by returning to the physical reasons for the exponential tail in the PDF. The XY model is diagonizable in reciprocal space reducing it to a model of statistically independent degrees of freedom: spin-wave amplitudes at wave vector $\mathbf{q}$, $\phi_{\mathbf{q}}$. The amplitudes $\langle \phi_{\mathbf{q}}^2 \rangle$ diverge at small q and are the modes that give the non-Gaussian fluctuations. In one dimension they completely destroy magnetic order, in two dimensions they give critical behavior, and between two and four dimensions they give remnant critical behavior in the form of a dangerously irrelevant variable.

II. PROBABILITY DENSITY FUNCTION FOR THE ORDER PARAMETER IN THE 2D XY MODEL

A. Analytic expression

The 2D XY model is defined by the Hamiltonian

$$H = -J \sum_{\langle i,j \rangle} \cos(\theta_i - \theta_j), \tag{5}$$

where the angles θ_i refer to the orientation of classical spins $\mathbf{S}_i$ confined in a plane and where the sum is over nearest-neighbor spins. In the following we consider a square lattice of side L, with periodic boundaries. The instantaneous magnetization is a two-dimensional vector $\mathbf{m}$ that, in zero field, is free to point in any direction. We define the order parameter as the scalar $m = |\mathbf{m}|$,

$$m = \frac{1}{N} \sum_{i=1}^{N} \cos(\theta_i - \overline{\theta}), \tag{6}$$

where $\overline{\theta} = \tan^{-1}(\Sigma_i \sin\theta_i / \Sigma_i \cos\theta_i)$ is the instantaneous magnetization direction. Within small corrections, which disappear in the thermodynamic limit, this corresponds to the more conventional definition

$$m = \frac{1}{N} \sqrt{\left(\sum_{i=1}^{N} \mathbf{S}_i \right)^2}.$$

For all temperatures below T_{KTB}, the renormalization-group trajectories flow, at large length scale, towards a regime where only spin-wave excitations are relevant [19,20]. The physics of the low-temperature phase is therefore completely captured by the quadratic Hamiltonian

$$H = \frac{J}{2} \sum_{\langle i,j \rangle} (\theta_i - \theta_j)^2. \tag{7}$$

We therefore restrict ourselves, in the following calculation, to this Hamiltonian and neglect the periodicity of the variables θ_i. Our calculation cannot therefore take into account the presence of vortex pairs. Close to T_{KTB} in two dimensions and also in one dimension, where free vortices are relevant variables, we would expect a deviation from the behavior shown in Fig. 2. This point is discussed further below.

We now calculate the PDF $P(m)$ that the system be in a state with magnetization m, using the standard property that a probability density function may be defined by the value of its moments [36]. Indeed, $P(m)$ can be expressed in terms of its characteristic function, $\tilde{P}(x)$:

$$P(m) = \int_{-\infty}^{\infty} \frac{dx}{2\pi} e^{imx} \tilde{P}(x), \tag{8}$$

which can in turn be expanded in a Taylor series whose coefficients are the moments $\langle m^p \rangle$:

$$\tilde{P}(x) = \sum_{p=0}^{\infty} \frac{x^p}{p!} \frac{\partial^p \tilde{P}}{\partial x^p}\bigg|_{x=0} = \sum_{p=0}^{\infty} \frac{(-ix)^p}{p!} \langle m^p \rangle, \tag{9}$$

so that

$$P(m) = \int_{-\infty}^{\infty} \frac{dx}{2\pi} e^{imx} \sum_{p=0}^{\infty} \frac{(-ix)^p}{p!} \langle m^p \rangle. \tag{10}$$

Equation (10) assumes that the series converges and that all the moments exists. Note that this last feature demands that $P(m)$ falls off faster than any power law of m.

The program for calculating $P(m)$ is therefore to calculate the moments $\langle m^p \rangle$, sum the series, and transform the final result. To this end it is useful to define the Green function in Fourier space,

$$G(\mathbf{q}) = \frac{1}{4 - 2\cos q_x - 2\cos q_y}, \tag{11}$$

where q_x and q_y take the discrete values $(2\pi/L)n$ of the Brillouin zone with $n = 0, \ldots, L-1$. We also define the set of constants $g_k = \Sigma_{\mathbf{q}} G(\mathbf{q})^k / N^k$. The value of g_1 diverges logarithmically with system size, illustrating the critical nature of the low-temperature phase [20,26]: $g_1 = (1/4\pi)\ln(CN)$, $C = 1.8456$ [37]. The values of g_k, $k \geqslant 2$ are independent of N in the thermodynamic limit. We find $g_2 \simeq 3.8667 \times 10^{-3}$, $g_3 \simeq 7.5719 \times 10^{-5}$, $g_4 = 1.7626 \times 10^{-6}$, and that for large k, g_k behaves like $(2\pi)^{1-2k}/2(k-1)$; see Appendix B.

The first moment is easily calculated within this approximation (see Appendix B and Refs. [26,14]). One finds that $\langle m \rangle$ decreases algebraically with the size, as one would expect from finite-size scaling [22],

$$\langle m \rangle = (NC)^{-k_B T/8\pi J}. \tag{12}$$

As discussed above, while the critical exponents β and ν are not individually defined for the 2D XY model, their ratio is defined [18] and the system obeys what Kosterlitz refers to as weak scaling [18]. Through Eq. (12), the ratio of exponents is defined: $\beta/\nu = \eta/2 = T/4\pi J$.

For higher moments we need a more systematic approach. A specific property of the quadratic Hamiltonian (7) is that the moments can be calculated using the tools of Gaussian integration [14,38]. In particular, by the application of Wick's theorem, propagators of order $2p$ in reciprocal space can be exactly expressed in terms of quadratic propagators so that the pth moment is proportional to $\langle m \rangle^p$. One finds [15,39]

$$\langle m^p \rangle = \langle m \rangle^p \frac{1}{(2N)^p} \sum_{\mathbf{r}_1, \ldots, \mathbf{r}_p} \sum_{\sigma_1, \ldots, \sigma_p = \pm 1} \times \exp\left[-\frac{\tau}{2} \sum_{i \neq j} \sigma_i G_R(\mathbf{r}_i - \mathbf{r}_j) \sigma_j \right], \tag{13}$$

where τ is the reduced temperature $k_B T/J$ and $G_R(\mathbf{r})$ the regularized Green function $\Sigma_{q \neq 0} G(\mathbf{q}) \exp(i\mathbf{q} \cdot \mathbf{r})/N$. In order to compute each moment of order p, we have to evaluate the sums over the positions and operators σ_i. The idea is to expand the exponential term (13) and introduce a diagrammatic representation of each quantity computed. For example, we represent $\sigma_i G_R(\mathbf{r}_i - \mathbf{r}_j)\sigma_j$ by a line between i and j on a lattice of p sites. The general term of the expansion is then a set of graphs with a combinatorial factor for the symmetries. Since $\sigma_i^2 = 1$, only closed diagrams are relevant, the factor 2^p being canceled by the sum over all the σ_i. The

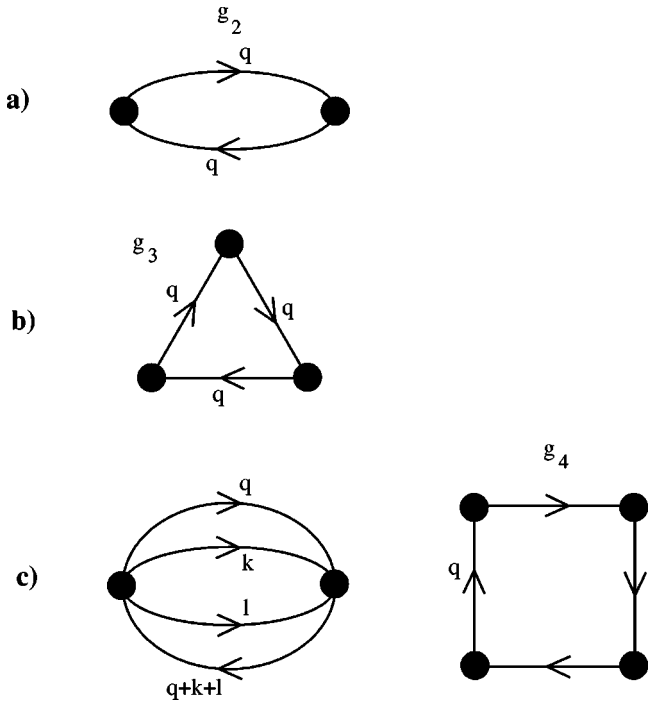

FIG. 1. Diagrams contributing to the distribution: (a) to order τ^2, (b) to order τ^3, and c) to order τ^4.

factor of τ^k is common to all graphs with k lines connected together, with an even connectivity at each vertex. For example, up to the second-order term in τ, we have

$$\langle m^p \rangle = \langle m \rangle^p \left[1 + \left(\frac{-\tau}{2} \right)^2 \frac{1}{2!} 2p(p-1) \frac{1}{N} \sum_{\mathbf{r}} G_R^2(\mathbf{r}) + \cdots \right]. \tag{14}$$

The term $\Sigma_{\mathbf{r}} G_R^2(\mathbf{r})/N^2 = \Sigma_{\mathbf{q} \neq \mathbf{0}} G(\mathbf{q})^2/N^2 = g_2$ is the value of the one loop graph with two lines, as shown in Fig. 1(a). There is an additional symmetry factor $2 \times p(p-1)$, which is the number of possible positions for such diagrams connecting two lines on a closed graph on a lattice of p points. For the third-order term in τ, we have only one diagram with three vertices, of value g_3, Fig. 1(b). The symmetry factor is equal to $p(p-1)(p-2) \times 4 \times 2$. The factor 4×2 comes from the number of possible ways of connecting three lines together. For the fourth-order term, there are three different graphs, two of which are shown in Fig. 1(c). The first has three loops and two vertices, the second, of value g_4, has one loop and four vertices. The third graph, not shown, consists of two disconnected one-loop graphs of the type shown in Fig. 1(a). In general, at each order in τ, we have the product of different closed diagrams, with one or many loops. It appears that the values of multiple-loop graphs, such as the first one in Fig. 1(c), are zero in the thermodynamic limit. We therefore find that only the one-loop diagrams are relevant and the value for such a diagram, with k lines and k vertices, is g_k. We can now express the pth moment of the magnetization as

$$\frac{\langle m^p\rangle}{\langle m\rangle^p}=1+\sum_{k\geqslant 2}\left(\frac{-\tau}{2}\right)^k\frac{1}{k!}\times\sum_{r\geqslant 1}\sum_{k_1+\cdots+k_r=k,k_i\geqslant 2}\times g_{k_1}\cdots g_{k_r}C(k_1,\ldots,k_r)\times p(p-1)\cdots(p-k+1), \tag{15}$$

with $C(k_1,\ldots,k_r)$ a combinatorial factor that takes into account the possible ways of putting together k lines on r graphs, the first with k_1 lines, the second with k_2 lines, etc., including the symmetries. For example, the factor associated with one triangle is $C(3)=4\times 2$. It is then relatively easy to show that

$$C(k_1,\ldots,k_r)=\frac{2^{k-r}k!}{(k_1+\cdots+k_r)(k_2+\cdots+k_r)\cdots k_r}. \tag{16}$$

Next, we can use the fact that every diagram is invariant by the action of the group $\mathcal{S}_r$ of permutations of its r single elements, so that, instead of Eq. (16), one can use a more convenient form for the combinatorial factor:

$$\frac{1}{r!}\sum_{\sigma\in\mathcal{S}_r}C(k_{\sigma(1)},\ldots,k_{\sigma(r)})=\frac{1}{r!}\frac{2^{k-r}k!}{k_1\cdots k_r}. \tag{17}$$

Setting $f_{k_i}=g_{k_i}(-\tau)^{k_i}/2k_i$, we arrive at the result

$$\begin{aligned}\frac{\langle m^p\rangle}{\langle m\rangle^p}&=1+\sum_{k\geqslant 2}\sum_{r=2}^{k}\frac{1}{r!}\sum_{k_1+\cdots+k_r=k}f_{k_1}\cdots f_{k_r}\times p(p-1)\cdots(p-k+1)\\&=1+\sum_{k\geqslant 2}\sum_{r=2}^{k}\frac{1}{r!}\sum_{k_1+\cdots+k_r=k}f_{k_1}\cdots f_{k_r}\frac{\partial^k}{\partial z^k}z^p\Big|_{z=1}\\&=\exp\left[\sum_{k=2}^{\infty}\frac{g_k}{2k}(-\tau)^k\partial_z^k\right]z^p\Big|_{z=1}.\end{aligned} \tag{18}$$

For $p=2$, we find $\langle m^2\rangle/\langle m\rangle^2=1+g_2\tau^2/2$ and defining $\sigma=\sqrt{\langle m^2\rangle-\langle m\rangle^2}$ we thus arrive at the hyperscaling condition that the ratio $\sigma/\langle m\rangle$ is independent of the system size. Hence

$$\sigma=\sqrt{\frac{g_2}{2}}\,\frac{k_BT}{J}\langle m\rangle. \tag{19}$$

One can now substitute for $\langle m^p\rangle$ in Eq. (10) using Eq. (18) and after rearranging the summations the distribution can finally be expressed as an integral, depending on the values of the one-loop diagrams g_k only,

$$P(m)=\int_{-\infty}^{\infty}\frac{dx}{2\pi}\exp\left[ix(m-\langle m\rangle)+\sum_{k=2}^{\infty}\frac{g_k}{2k}(i\tau\langle m\rangle x)^k\right].$$

Changing variables, $x\to x/\sigma$, and using Eq. (19) we find

$$P(m)=\int_{-\infty}^{\infty}\frac{dx}{2\pi\sigma}\exp\left[ix\frac{m-\langle m\rangle}{\sigma}+\sum_{k=2}^{\infty}\frac{g_k}{2k}\left(ix\sqrt{\frac{2}{g_2}}\right)^k\right], \tag{20}$$

which is the principal result of Ref. [15]. Defining $\sigma P(m)=\Pi(\theta)$, we see that the function Π depends uniquely on the variable $\theta=(m-\langle m\rangle)/\sigma$ and the g_k, $k\geqslant 2$. As the g_k are constants in the thermodynamic limit, $\Pi(\theta)$ is a universal function, independent of both system size and temperature. The asymmetry comes from the fact that the ratios $g_k/(g_2/2)^{k/2}$, $k\geqslant 3$ are nonzero and this constitutes the abnormal influence of the integral scale. If, in the thermodynamic limit, $k=2$ were the only nonzero term, one would arrive at a Gaussian PDF centered on $\langle m\rangle$. Departure from a Gaussian function is typically characterized by the skewness, $\gamma=\langle\theta^3\rangle$, and kurtosis, $\kappa=\langle\theta^4\rangle$ [40]. We find

$$\gamma=-\frac{g_3}{(g_2/2)^{3/2}}=-0.8907, \tag{21}$$

$$\kappa=3+3\frac{g_4}{(g_2/2)^2}=4.415.$$

Although we can calculate the asymptotic behavior of g_k for large k, we are not able to compute the constants analytically and so we cannot sum the series (20). However, we can transform it into a very much more useful form by keeping N large but finite and inverting the sums over $\mathbf{q}$ and k. The even and odd terms are separated and summed independently and we eventually find

$$\Pi(\theta)=\int_{-\infty}^{\infty}\sqrt{\frac{g_2}{2}}\frac{dx}{2\pi}\exp\left\{ix\theta\sqrt{\frac{g_2}{2}}-\sum_{\mathbf{q}\neq\mathbf{0}}\left[\frac{i}{2}xG(\mathbf{q})/N-\frac{i}{2}\arctan(xG(\mathbf{q})/N)+\frac{1}{4}\ln[1+x^2G(\mathbf{q})^2/N^2]\right]\right\}. \tag{22}$$

The sum over $\mathbf{q}$ and the integral over x in Eq. (22) can now be performed numerically, allowing the evaluation of $\Pi(\theta)$.

B. Comparison with simulation

To test the above calculation and to verify its scaling properties, we have carried out extensive numerical simulations of the 2D XY model with full cosine interaction, Eq. (5), for different values of temperature and system size. In addition, we have also done microcanonical molecular-dynamics (MD) simulations to check the possible dependence of the PDF for fluctuations on the statistical ensemble.

The Monte Carlo simulations were performed with 10^8 Monte Carlo steps per spin, with 10^6 steps used for equilibration. The MD simulation was carried out for systems of N classical rotators [41], with Hamiltonian

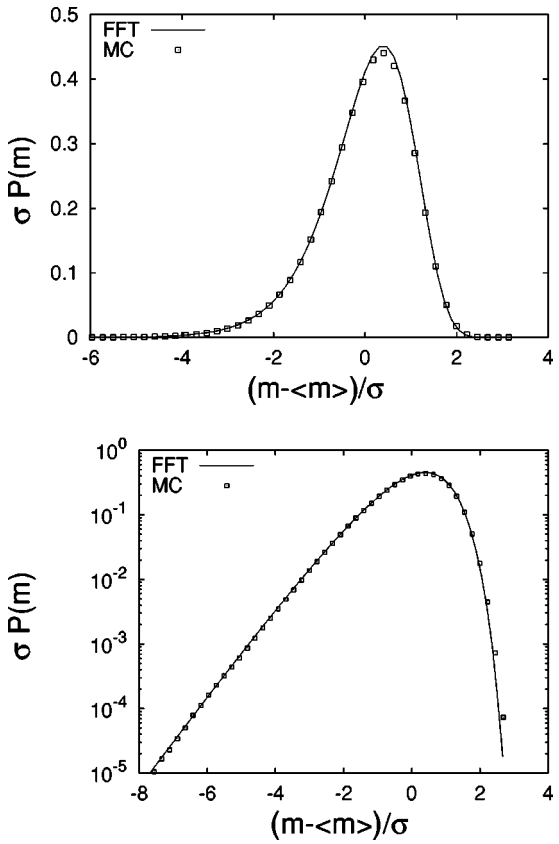

FIG. 2. The PDF, as obtained from a fast Fourier transform (FFT) of Eq. (22), compared with MC simulation of a 2D XY model at temperature $T=0.1$ of size $N=32^2$ (upper: natural scale; lower: semilog scale).

$$H_R=\sum_{i=1}^{N}\frac{\dot{\theta}_i^2}{2}+J\sum_{\langle ij\rangle}[1-\cos(\theta_i-\theta_j)]. \tag{23}$$

The equations of motion were integrated numerically, using a Verlet algorithm. In order to explore the low-temperature fluctuation regime, the initial configuration of the system was chosen with the spins pointing in the same direction and with a Gaussian distribution of momenta. The system was then equilibrated for a time of 10^6-10^7 sweeps and data collected over a time span of 10^8-10^9 sweeps according to the size of the system. Note that one cannot use the harmonic interaction (7) to study deterministic dynamics in the microcanonical ensemble, as this would allow no coupling between the spin-wave modes and no evolution would be possible. The nonlinearity of the cosine interaction allows mixing between the normal modes and the sampling of equilibrium states. Here we do not report work at high enough energies to allow vortex formation [42,43] with any significant probability. Rather, the nonlinearity plays the role of the heat bath in the canonical ensemble, while the physics is still correctly described by the harmonic part of the interaction.

The numerical integration of Eq. (22), performed with a fast Fourier transform (FFT) algorithm [44], is shown in Fig. 2, where it is compared with Monte Carlo results for $T/J=0.1$ and $N=32^2$. The theoretical curve is clearly in extremely good agreement with the numerical data. The curve is asymmetric, with what appears to be an exponential tail for fluctuations below the mean and a much more rapid fall off in amplitude for fluctuations above the mean.

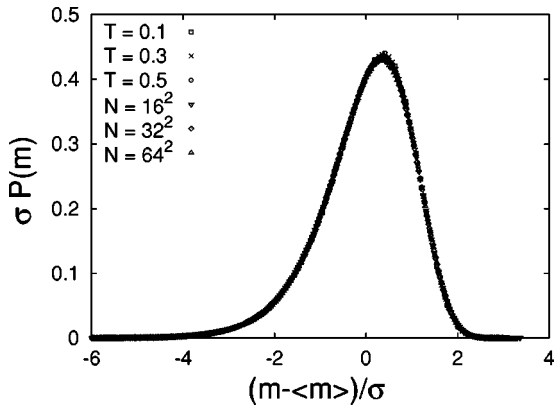

FIG. 3. The PDF for fluctuations in dimension $D=2$ from MC and MD simulations. The first set of data corresponds to canonical MC simulation for a system of size $N=32^2$ at temperature $T=0.1$, 0.3, 0.5. The second set of data corresponds to microcanonical MD simulation at temperature $T\simeq 0.7$ and size $N=16^2$, 32^2, 64^2.

In Fig. 3, we show the PDF for fluctuations in m obtained from MC simulation for fixed system size and varying temperature, as well as MD for fixed temperature and different system sizes. The result of Ref. [11] and Sec. II of this paper is that, for the harmonic Hamiltonian, Eq. (7), $\Pi(\theta)$ is independent of both system size and temperature, while we have explicitly tested this result against the PDF generated for the full Hamiltonian, Eq. (5). Qualitative agreement is clearly excellent, independent of the ensemble used, but there are small systematic deviations in the tails, when observed on a logarithmic scales [45], as shown in Figs. 4 and 5. We can only expect agreement between the analytic result and simulation in the range of temperature sufficiently below T_{KTB} such that vortex pairs do not influence the PDF [14]. Even in the absence of vortices, one must expect small variations

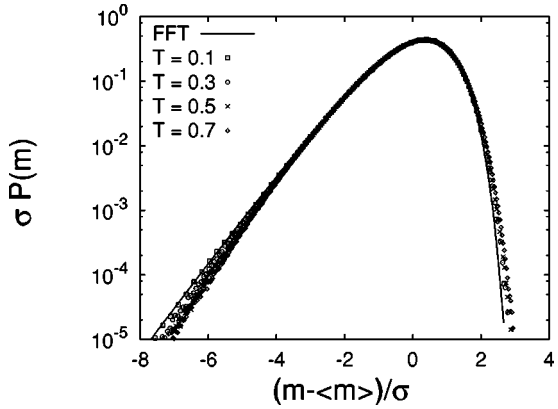

FIG. 4. The PDF, as obtained from a fast Fourier transform (FFT) of Eq. (22), in dimension $D=2$ compared with Monte Carlo results for a system of size $N=32^2$ at temperature $T=0.1$, 0.3, 0.5, 0.7.

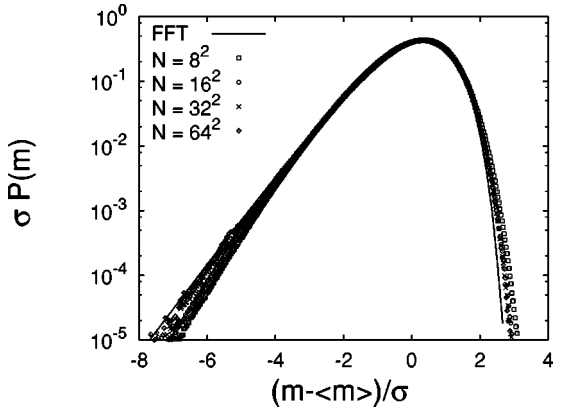

FIG. 5. The PDF, as obtained from a fast Fourier transform (FFT) of Eq. (22), in dimension $D=2$ compared with MD results for a system of size $N=8^2$, 16^2, 32^2, 64^2 at temperature $T\simeq 0.7$.

from our theoretical result for small system sizes that stem from the utilization of Eq. (5) rather than Eq. (7). In a renormalization-group treatment, the nonlinearities of Hamiltonian (5) scale away on changing the length scale and the Hamiltonian is replaced by an effective harmonic Hamiltonian at higher temperature [20]. For example, at $T/J=0.7$, for $L=32$, we find $\langle m\rangle=0.76$ from simulation, while Eq. (12) gives $\langle m\rangle=0.81$. The effective coupling constant can be calculated by expanding the cosine and approximating the nonlinear terms using a Hartree approximation [19]. Renormalization of the nonlinearities introduces a microscopic length scale a' that gives small corrections when compared with the calculated PDF. However, this length scale is fixed by the temperature and the corrections should scale away as the ratio $a'/L\to 0$. This scenario is confirmed in Fig. 5, where data are shown at $T/J=0.7$ for $L=8$, 16, 32, and 64 and are compared with the theoretical curve. Deviations from the theoretical result are observed for $L=8$ and $L=16$ but the PDF clearly approaches the predicted scale independence for the larger system sizes.

Near T_{KTB}, vortices influence the PDF, however the vortex population decreases exponentially moving away from T_{KTB} [42] and they only make their presence felt within the physical domain in a small band of temperatures near the transition. In this regime, the data do not fit on the universal curve [14,43,45], but a detailed discussion of this point is outside the scope of this paper.

C. $P(m)$ for the linearized order parameter

As Eq. (22) is independent of temperature, one should be able to obtain it at low temperature where the magnetization is approximately

$$m=1-\frac{1}{2N}\sum_i\ (\theta_i-\overline{\theta})^2. \tag{24}$$

In fact, using this expression one can arrive at Eq. (22) in a more straightforward manner. What is perhaps surprising is that the calculation, using Eq. (24), is valid for all temperatures below T_{KTB}, even for temperatures where Eqs. (6) and (24) represent different physical quantities.

Using the Hamiltonian (7), we have

$$P(m)=\frac{1}{Z}\int_{-\infty}^{\infty}\frac{dx}{2\pi}\int\prod_i\ d\theta_i\exp\left\{ix\left[m-1+\frac{1}{2N}\sum_i\ \theta_i^2\right]-\frac{1}{2\tau}\sum_{i,j}\ \theta_i G_{ij}^{-1}\theta_j\right\},$$

where G_{ij}^{-1} is the inverse Green's-function operator connecting sites i and j with nonzero elements for i and j nearest neighbors [16], and $Z=(\det G^{-1}/2\pi\tau)$ is the partition function.

It is easy to integrate the Gaussian integral by transforming into reciprocal space. Defining the trace Tr of any function of G as the sum for $\mathbf{q}\neq\mathbf{0}$ of the same function of $G(\mathbf{q})$ and using $\langle m\rangle=1-\tau\,\mathrm{Tr}\,G/2N$, we find

$$P(m)=\int_{-\infty}^{\infty}\frac{dx}{2\pi}\exp\left[ix(m-\langle m\rangle)-ix\frac{\tau}{2}\,\mathrm{Tr}\,G/N-\tfrac{1}{2}\mathrm{Tr}\ln(\mathbf{1}-ix\tau G/N)\right]. \tag{25}$$

We can now use the fact that $\sigma=\sqrt{g_2/2}\tau$ in this approximation, to transform Eq. (25) into a dimensionless and universal form,

$$\Pi(\theta)=\int_{-\infty}^{\infty}\sqrt{\frac{g_2}{2}}\frac{dx}{2\pi}\exp\left[ix\theta\sqrt{\frac{g_2}{2}}-i\frac{x}{2}\,\mathrm{Tr}\,G/N-\frac{1}{2}\,\mathrm{Tr}\ln(\mathbf{1}-ixG/N)\right]$$
$$=\int_{-\infty}^{\infty}\sqrt{\frac{g_2}{2}}\frac{dx}{2\pi}\exp[i\Phi(x)], \tag{26}$$

which is the same expression as Eqs. (20) and (22), once we separate the real and imaginary parts of the integrand. This demonstration proves that the only relevant graphs are those with only one loop, the others being zero in the thermodynamic limit.

Within this linear approximation, the mean magnetization $\langle m\rangle$ and the standard deviation σ do not scale in the same way with system size: while $\langle m\rangle=1-(T/8\pi J)\ln(CN)$, $\sigma=\sqrt{g_2/2}\tau$ is a temperature-dependent constant. This exact result can be verified by applying Eq. (9) to Eq. (25) and calculating $\langle m\rangle$ and $\langle m^2\rangle$ directly. The fact that we find the same universal function for the two calculations, when written in the form (2), shows explicitly that the hyperscaling result $\sigma/\langle m\rangle\sim O(1)$ is not a necessary condition for non-Gaussian data collapse. Rather, it seems that hyperscaling is a consequence, in these circumstances, of the correct definition of m as an order parameter on the interval [0,1].

The Gaussian limit of the 2D XY model is identical to the Edwards-Wilkinson (EW) model of interface growth and the linear approximation for the order parameter is related to the

square of the interface width $m=1-w^2$. The PDF for w^2 has been studied in one [28] and two [24] dimensions together with extensions to the EW model, including nonlinearity [46,47]. All models give non-Gaussian PDF's with the same qualitative features as Fig. 2. These models provide an important microscopic link between equilibrium and nonequilibrium systems and suggest that a formalism could exist that incorporates the statistical features that we have observed to be shared, at a global level, between such different systems.

D. Asymptotes of $\Pi(\theta)$ for large fluctuations

As a first step towards an analytic form for $\Pi(\theta)$, one can approximate Eq. (22) beyond the Gaussian approximation by retaining only the elements (g_2,g_3). In this case, the solution is proportional to the Airy function

$$\Pi(\theta)\propto\exp\left(-\frac{1}{6\alpha}\theta\right)\mathrm{Ai}\left[\frac{1}{(3\alpha)^{1/3}12\alpha}-\frac{1}{(3\alpha)^{1/3}}\theta\right], \tag{27}$$

where $\alpha=2^{3/2}g_3/3g_2^{3/2}\simeq 0.296\,876$. The g_3 term assures that it is not symmetric on reversing the sign of θ. We find that the approximation reproduces qualitatively the apparent exponential behavior for $\theta\ll -1$:

$$\Pi(\theta)\sim\left\{2\sqrt{\pi}\left[\frac{1}{(3\alpha)^{1/3}12\alpha}-\frac{1}{(3\alpha)^{1/3}}\theta\right]^{1/4}\right\}^{-1}\times\exp\left\{-\frac{1}{6\alpha}\theta-\frac{2}{3}\left[\frac{1}{(3\alpha)^{1/3}12\alpha}-\frac{1}{(3\alpha)^{1/3}}\theta\right]^{3/2}\right\}. \tag{28}$$

However, the approximation does not allow us to extract the asymptote above the mean, as for $\theta>0$ the Airy function develops oscillations.

A more fruitful approach is to look at the saddle points of the integrand (22), from which one can extract both asymptotes. If $\theta\ll -1$, an expansion near $x=0$ is not very satisfactory and we must rather seek the solution for the extrema of the whole integrand, $\partial\Phi(x)/\partial x=0$. We find

$$\sqrt{\frac{g_2}{2}}\theta=\tfrac{1}{2}\mathrm{Tr}\,\frac{G^3}{N^3}\,\frac{x^2}{1+x^2G^2/N^2}-\frac{i}{2}\mathrm{Tr}\,\frac{G^2}{N^2}\,\frac{x}{1+x^2G^2/N^2}. \tag{29}$$

If θ is negative and x real, the real part of the second term is always positive and there is no solution to this equation. We therefore seek a solution for x pure complex, $x=iy$. In this case, Eq. (29) becomes

$$\sqrt{\frac{g_2}{2}}\theta=\tfrac{1}{2}\mathrm{Tr}\,\frac{G^2}{N^2}\,\frac{y}{1+yG/N}=\varphi(y). \tag{30}$$

The function φ has simple poles at $y=-4\pi^2,-8\pi^2,-32\pi^2,\ldots$ and its asymptotic value near the first pole $y_0=-4\pi^2$ is $\varphi(y)\sim -2/(y-y_0)$. The extremum of the integrand satisfies the condition $y^*\simeq y_0-2\sqrt{2/g_2}/\theta>y_0$ for $|\theta|$ large and we can deform the real path of the integration so that it passes through the extremum on the imaginary axis. Near the extremum, we can expand the integrand up to second order in $y-y^*$ and perform a Gaussian integration:

$$\Pi(\theta)\simeq\int_{-\infty}^{\infty}\sqrt{\frac{g_2}{2}}\frac{dx}{2\pi}\exp[i\Phi(iy^*)+i\tfrac{1}{2}(x-iy^*)^2\Phi''(iy^*)]. \tag{31}$$

We finally find that the asymptotic value of the distribution varies as

$$\Pi(\theta)\propto|\theta|\exp\left(4\pi^2\sqrt{\frac{g_2}{2}}\theta\right). \tag{32}$$

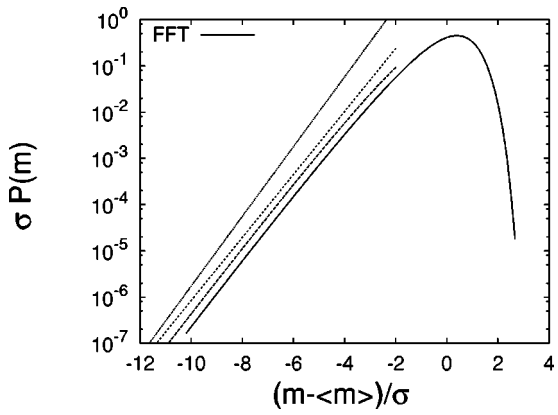

FIG. 6. Comparison of the tail of the PDF with the exact asymptote (long dashed), Eq. (32), the true exponential tail of slope $4\pi^2\sqrt{g_2/2}\simeq 1.736$ (dotted), and an effective exponential tail of slope $\alpha=1.568\,67\ldots$ (short dashed). The curves are displaced from each other for clarity.

We have superimposed the asymptotic result (32) and the full numerical integration for $N=101^2$ of Eq. (22) in Fig. 6. The amplitude of Eq. (32) is chosen so that the curves are slightly displaced to allow comparison of the slopes. The asymptotic solution is in excellent agreement even for θ values where the PDF shows a distinct deviation away from exponential behavior and only fails for $\theta>-2$. Further out in the tail, in the range $-10<\theta<-4$, $\ln(\Pi)$ is approximately linear. However, the value of the slope is not the argument of the exponential in Eq. (32), $4\pi^2\sqrt{g_2/2}\simeq 1.736$. The logarithmic corrections given by the term $|\theta|$ are significant over the whole of this range, but the curvature is so small that the data can be fitted to an effective exponential $\Pi(\theta)\sim\exp(\alpha\theta)$, with $\alpha=1.568\,67\ldots$. The data only approach true exponential behavior for $\theta<-30$, which is completely outside any imaginable physical range. Strictly speaking, it is therefore more correct to speak of pseudoexponential, $x\exp(\alpha x)$, for the asymptote below the mean.

For large and positive θ, a solution of Eq. (30) exists for large and positive y. A reasonable approximation is to replace G by $1/q^2$ and perform the integration

$$\varphi(y) \sim \frac{1}{2}\int_{q=2\pi/\sqrt{N}}^{2\pi} \frac{Nd^2q}{4\pi^2}\frac{1}{N^2q^4}\frac{y}{1+y/Nq^2}$$

$$\sim \frac{1}{4\pi}\int_{2\pi/\sqrt{y}}^{\infty}\frac{dq}{q(1+q^2)} \sim \frac{1}{8\pi}\ln y. \tag{33}$$

A more precise computation gives $\varphi = \ln(y)/8\pi + \hat{a} + 1/2y + \cdots$, where $\hat{a}$ is a numerical constant that can be computed exactly. An analytical study (see Appendix C) gives

$$\hat{a} = \frac{1}{24} + \frac{\gamma}{4\pi} - \frac{1}{4\pi}\ln(4\pi) - \frac{1}{2\pi}\ln\prod_{k=1}^{\infty}[1-\exp(-2\pi k)]$$

$$= -0.113\,514\,443\,37\ldots. \tag{34}$$

For large θ, the saddle point of the integrand is therefore located at $y^* = \exp 8\pi(-\hat{a} + \sqrt{(g_2/2)}\,\theta)$, and the asymptotic value for Π follows from a Gaussian integration of Eq. (31):

$$\Pi(\theta) \propto \exp\left[-\frac{1}{8\pi}e^{8\pi(\sqrt{(g_2/2)}\theta - \hat{a})} + 8\pi\sqrt{\frac{g_2}{2}}\theta\right]. \tag{35}$$

Comparing the asymptote with the full curve, we again find that the true asymptote only fits accurately outside the physical domain, although the data are clearly consistent with a very rapid fall off in the PDF for θ above the mean.

III. FITTING TO KNOWN FUNCTIONAL FORMS

The obvious question now arises: is the PDF generated by the characteristic function (22) of known functional form? We do not have a definitive answer to this question, as we are not able to transform Eq. (22) analytically. In the absence of an answer, we test the PDF against three skewed functions, shown in Eq. (4), which describe statistics in different physical situations. These are a modified Gumbel function, characteristic of problems where extreme values dominate the sum over many contributions; a log-normal distribution, characteristic of statistically independent multiplicative processes; and a χ^2 distribution that describes the PDF of a quantity made up of a finite number of positive-definite microscopic variables. The analysis is the same in all three cases, but is only shown in detail for the modified Gumbel function: each curve has four parameters, but once the value of the first is chosen, the others are fixed by normalization and the constraints $\langle\theta\rangle = 0$, $\langle\theta^2\rangle = 1$. The family of one-parameter curves are Fourier-transformed and the first four terms in a Taylor expansion are set equal to those for the generating function, which fixes the value of the free parameter. The method takes into account the skewness of the curve but not the kurtosis, and its accuracy is ultimately limited. The goodness of fit can be measured by comparing the ratio of higher-order terms of the expansion of the test and generating functions. For an exact solution, all higher ratios would be equal to unity, while for a poor fit they diverge rapidly from this value. Other functions could be tested in the same way and an exact solution, unknown to us, may well exist in the statistics literature.

The method described above is quite similar to that due to Pearson [48], who realized a century ago that, in many practical situations, knowledge of the first four moments of a distribution is sufficient to generate a curve, fitting any set of data points [51]. Pearson developed a phenomenological differential equation containing the numerical values of the moments, whose solution gives the fitting function. A Pearson analysis is performed on the calculated PDF at the end of the section.

A. The generalized Gumbel distribution

The asymptotes (32) and (35) are of the same general form as those for Gumbel's first asymptote distribution from the theory of extremal statistics [32]: defining z to be the ath largest value from a set of z_i, $i = 1,N$ random numbers taken from a generator $f(z)$, the PDF for z is

$$g_a(z) = \frac{a^a\alpha_a}{\Gamma(a)}\exp\{-a[\alpha_a(z-u_a) + e^{-\alpha_a(z-u_a)}]\}. \tag{36}$$

$\Gamma(a)$ is the gamma function; u_a is the value of z such that a of the N random numbers are greater than z. $F(z)$ is the probability of having a of the values less than z, such that $F(u_a) = 1 - a/N$. α_a is referred to as the intensity: $\alpha_a = (N/a)f(u_a)$. In conventional statistics, a would of course be an integer. However, in what follows we are going to see an irrational number appearing.

The function (36) has an exponential tail for fluctuations towards large values of z, the opposite of the PDF, in Fig. 2. We therefore make a change of variables $m_z = 1 - z$, $\theta_z = (m_z - \langle m_z\rangle)/\sigma_z$, which makes a mirror reflection of Eq. (36). Within the linear approximation for the order parameter, this corresponds to the relevant variable being the sum of the spin-wave amplitudes $z \to (1/2N)\Sigma_i(\theta_i - \overline{\theta})^2$ [21,50]. Changing variables, we find

$$\sigma_z\Pi_G(\theta_z) = we^{ab(\theta_z - s) - ae^{b(\theta_z - s)}},$$

$$b = \alpha_a\sigma_z,$$

$$s = (1 - \langle m_z\rangle - u_a)/\sigma_z, \tag{37}$$

$$w = \frac{a^a\alpha_a}{\Gamma(a)}\sigma_z.$$

Equation (37) is also the distribution for the ath smallest random number from the set z_i. After some algebra, one can show that

$$b = \sqrt{\frac{1}{\Gamma(a)}\frac{\partial^2\Gamma(a)}{\partial a^2} - \left[\frac{1}{\Gamma(a)}\frac{\partial\Gamma(a)}{\partial a}\right]^2},$$

$$s = \frac{1}{b}\left[\ln(a) - \frac{1}{\Gamma(a)}\frac{\partial\Gamma(a)}{\partial a}\right]. \tag{38}$$

Now rewriting Eqs. (32) and (35), one finds

$$\Pi(\theta)\propto\begin{cases}|\theta|\exp\left(\dfrac{\pi}{2}b\,\theta\right), & \theta\ll 0\\[2ex] \exp\left(-\dfrac{\pi}{2}e^{b(\theta-s)}+c\,\theta\right), & \theta\gg 0,\end{cases}\tag{39}$$

with $b=8\pi\sqrt{g_2/2}\simeq 1.105$, $s=0.745$, and $c=b$. These asymptotes differ only slightly from those for a generalized Gumbel function with $a=\pi/2$, first through the term $|\theta|$ for fluctuations below the mean and second through the term $\exp(c\theta)$ above the mean: the coefficient $c=(\pi/2)b$ for the modified Gumbel function, while $c=b$ for the true asymptote. These differences are enough to ensure that the modified Gumbel equation is not an exact solution to Eq. (20), however the comparison is so close that it is tempting to try to get a good fit to Eq. (22) by solving for the constants a, b, s, and w.

Fourier transforming Eq. (37) gives

$$\begin{aligned}\Pi_G(\theta)&=\int_{-\infty}^{\infty}\frac{dx}{2\pi}\frac{w}{b}\exp\left(ix\theta-isx+i\frac{x}{b}\ln a-a\ln a\right)\\&\quad\times\Gamma\left(a-i\frac{x}{b}\right)\\&=\int_{-\infty}^{\infty}\frac{dx}{2\pi}\exp[i\Phi_G(x)].\end{aligned}\tag{40}$$

We can compare $\Phi_G(x)$ with $\Phi(x\sqrt{2/g_2})$, assuming that the two Fourier transforms are nearly equal. The four constants should be calculated by minimizing the difference between the two functions. To do this, we can set the first four coefficients of the Taylor expansion of these functions equal. For $\Phi_G(x)$, we have

$$\begin{aligned}\Phi_G(x)&=ia\ln a-i\ln(w/b)-i\ln\Gamma(a)\\&\quad+[-s-\Psi(a)/b+\ln(a)/b]x+\frac{i}{2b^2}\Psi'(a)x^2\\&\quad+\frac{1}{6b^3}\Psi''(a)x^3-\frac{i}{24b^4}\Psi'''(a)x^4\\&\quad-\frac{1}{120b^5}\Psi^{(4)}(a)x^5+\cdots,\end{aligned}\tag{41}$$

where $\Psi(z)$ is the digamma function $\Gamma'(z)/\Gamma(z)$. For Φ, we have

$$\Phi(x\sqrt{2/g_2})=\frac{i}{2}x^2-\frac{\sqrt{2}g_3}{3g_2^{3/2}}x^3-i\frac{g_4}{2g_2^2}x^4+\frac{2\sqrt{2}g_5}{5g_2^{5/2}}x^5+\cdots.\tag{42}$$

We therefore find that the four constants satisfy the relations

$$\frac{b}{w}=\frac{\Gamma(a)}{a^a},\quad sb=\ln a-\Psi(a),\tag{43}$$

$$b^2=\Psi'(a),\quad b^3g_3\left(\frac{2}{g_2}\right)^{3/2}=-\Psi''(a).$$

The first three equations arise from the constraints of normalization of the distribution, while the last expresses these constraints in terms of g_2 and g_3. The equations can be solved numerically. We find

$$\begin{aligned}a&=1.580\,680\,1,\quad b=0.933\,935\,5,\\s&=0.373\,179\,2,\quad w=2.160\,285\,8.\end{aligned}\tag{44}$$

The constants b and s calculated in this way are shifted slightly from the values extracted from the asymptotes, but a is close to our very appealing first try, $\pi/2$. Taking this value and calculating the constants b, s, and w from normalization, one finds

$$\begin{aligned}a&=\pi/2,\quad b=0.938,\\s&=0.374,\quad w=2.14,\end{aligned}\tag{45}$$

in very satisfying agreement with the first method of calculation.

Given this solution, we can compute the coefficient ratio for the higher-order terms in Eqs. (41) and (42):

$$\frac{1}{\Phi_G^{(4)}(0)}\frac{\partial^4\Phi(x\sqrt{2/g_2})}{\partial x^4}\bigg|_{x=0}=\frac{12g_4b^4}{g_2^2\Psi'''(a)}=0.926\,502\,9,\tag{46}$$

$$\frac{1}{\Phi_G^{(5)}(0)}\frac{\partial^5\Phi(x\sqrt{2/g_2})}{\partial x^5}\bigg|_{x=0}=-\frac{48\sqrt{2}g_5b^5}{g_2^{5/2}\Psi^{(4)}(a)}=0.826\,742\,9.\tag{47}$$

The ratio of coefficients clearly diverges from unity, but it does so slowly, indicating that the modified Gumbel function should be a good fit to the curve over the physical range. This is confirmed in Fig. 7, where we compare Eq. (37), using the values (44), with the exact result, from Eq. (22). On a natural scale, the agreement is remarkably good over the entire range, with the only visible deviation coming around the maximum of the PDF, where the Gumbel curve is very slightly lower. On a logarithmic scale there is excellent general agreement over the whole of the plotted range, but a slight deviation can be observed for probabilities below 10^{-3}. For fluctuations below the mean, the deviation is because the true asymptotic behavior is quasiexponential, $x\exp(-\alpha x)$, and has a slight curvature, as discussed in the preceding section. The results therefore confirm that, although the generalized Gumbel function is an excellent approximation for the PDF (22), it is not an exact solution.

From these results it is very tempting to take the generalized Gumbel function, with a exactly $\pi/2$ as a working analytic expression for the PDF. However the connection with extremal statistics remains an open question [34]. As discussed in Sec. V, the spin-wave Hamiltonian (7) is diagonalized in reciprocal space and the problem can be formulated in terms of a set of statistically independent variables. The

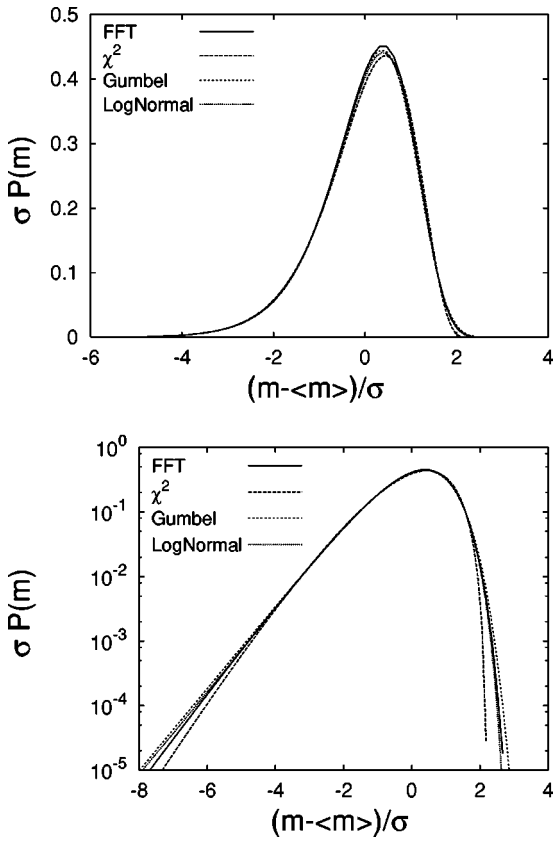

FIG. 7. The PDF compared with the generalized Gumbel, log-normal, and χ^2 functions described in the text.

PDF for extreme values of statistically independent variables can only follow three different asymptotic [32,40] or limit functions as the thermodynamic limit is taken. The only possible limit functions from extremal statistics of the Gumbel form discussed here are for a integer, with $a=1$ for the biggest or smallest values.

Chapman *et al.* [34] have recently argued that the PDF for global quantities in any system with identifiable excitations on scales up to the system size should be dominated by extreme values. They showed that the PDF of extreme values among 10^5 Gaussian random number generators approximates to a Gumbel function with $a=\pi/2$. This is not one of the predicted asymptotes [40], and we suggest that the deviation must be due to a very slow approach to the limit function with system size. It therefore does not seem to be a correct description of the 2D XY data as we do have a limit function that is well represented by Eq. (37) with $a=\pi/2$. However, if the results of [34] are relevant for nonequilibrium phenomena such as turbulence and self-organized criticality, it would suggest the interesting property that corrections to the asymptotic forms, or limit functions, are a generic feature of these systems.

B. Generalized log-normal distribution

The generalized log-normal distribution has the form

$$\Pi_L(\theta)=\frac{w}{\sqrt{2\pi\sigma_L^2(s-\theta)}}\exp\left\{-\frac{1}{2\sigma_L^2}[\ln(s-\theta)-a]^2\right\}, \tag{48}$$

with $w=1$. Following the same procedure as before, the generating function $\Phi_L(x)$ can be developed as a power series,

$$\Phi_L(x)=x(\theta-s+e^{a+\sigma_L^2/2})+i\frac{x^2}{2}(e^{2a+2\sigma_L^2}-e^{2a+\sigma_L^2}) -x^3(\tfrac{1}{6}e^{3a+9\sigma_L^2/2}+\tfrac{1}{3}e^{3a+3\sigma_L^2/2}-\tfrac{1}{2}e^{3a+5\sigma_L^2/2}). \tag{49}$$

Comparing Eq. (49) with Eq. (42), one finds the following expressions for s, a, and σ_L:

$$s=e^{a+\sigma_L^2/2},$$

$$a=-\tfrac{1}{2}\ln(e^{2\sigma_L^2}-e^{\sigma_L^2}), \tag{50}$$

$$\frac{\sqrt{2}}{3}\frac{g_3}{g_2^{3/2}}=\tfrac{1}{6}e^{3a}(e^{9\sigma_L^2/2}+2e^{3\sigma_L^2/2}-3e^{5\sigma_L^2/2}).$$

Eliminating a and σ_L leads to a cubic equation for s in terms of $\alpha=(g_2/2)^{3/2}/g_3=1/|\gamma|$:

$$s^3-3\alpha s^2-\alpha=0, \tag{51}$$

which could be solved exactly. We have solved it numerically, verifying that there exists one real and two complex roots. We find

$$s=3.459\,81, \quad a=1.201\,09, \quad \sigma_L=0.283\,25.$$

The function, with these parameters, is compared with the calculated PDF in Fig. 7. The general quality of fit is again excellent over the plotted range, with very small systematic deviations occurring in the wings of the distribution. It does not have the correct asymptotes, either exponential on the left or double exponential on the right, but as we have shown in the preceding section, the true asymptotic behavior is only reached outside the plotted regime, which explains why such a good fit can be achieved.

We have not, for the moment, been able to develop a physical reasoning associated with the log-normal function and the origin, $s=3.4$, although related to γ, seems rather arbitrary, but we do not exclude an explanation in terms of random multiplicative processes. Note that log-normal distribution does appear in surface dynamics. Namely, starting with a flat interface as an initial condition, the short-time limit of the $D=1$ Edwards-Wilkinson dynamics yields a log-normal distribution for the interface width [66].

C. Generalized χ^2 distribution

The χ^2 distribution for ν statistically independent degrees of freedom has the form

$$\Pi_\chi(\theta)=w(s-\theta)^{\nu/2-1}e^{-a(s-\theta)}, \tag{52}$$

with

$$w=\frac{a^{\nu/2}}{\Gamma(\nu/2)},$$
$$\nu=2a^2. \tag{53}$$

As in the case of the Gumbel function, the generating function can be found in closed form:

$$\Phi_\chi(x)=x(\theta-s)+i\frac{\nu}{2}\ln(1-ix/a), \tag{54}$$

whose development up to fourth order in x leads to

$$\Phi_\chi(x)=x(\theta-s)+\frac{\nu}{2a}x+i\frac{\nu}{4a^2}x^2-\frac{\nu}{6a^3}x^3-i\frac{\nu}{8a^4}x^4 + O(x^5)+\cdots. \tag{55}$$

This series can again can be compared with Eq. (42) to give

$$s=\frac{\nu}{2a},$$
$$a=\sqrt{\frac{\nu}{2}}=s, \tag{56}$$
$$\nu=\frac{g_2^3}{g_3^2}=\frac{8}{\gamma^2},$$

with numerical values

$$\nu=10.071\,55,\quad a=2.244\,05,\quad s=a,\quad w=2.312\,33.$$

Comparing the function shown in Fig. 7 with these parameters with the calculated curve, there is reasonably good agreement but this time deviation can be seen when plotted both on a real and a logarithmic scale. On the logarithmic scale, the deviation is stronger than for the other fitting functions.

One can see that describing the correlated system as a finite number of degrees of freedom is a reasonably good approximation. It is an appealing concept and the calculation yields a system-size-independent number that depends uniquely on the skewness: $\nu=g_2^3/g_3^2=8/\gamma^2$. If γ developed towards zero, then ν would diverge and the χ^2 interpretation would be consistent with a Gaussian distribution. However, quantitatively it is not correct and the true description is a many-body one [52]. The difference between the two curves can be quantified by considering the ratio of the fourth-order terms:

$$\Phi_\chi(x)^{(4)}=-i\frac{1}{2\nu},$$
$$\Phi(x)^{(4)}=-i\frac{g_4}{2g_2}, \tag{57}$$

so that $\Phi(x)^{(4)}/\Phi_\chi(x)^{(4)}\sim 0.0238$, which is very far from 1.

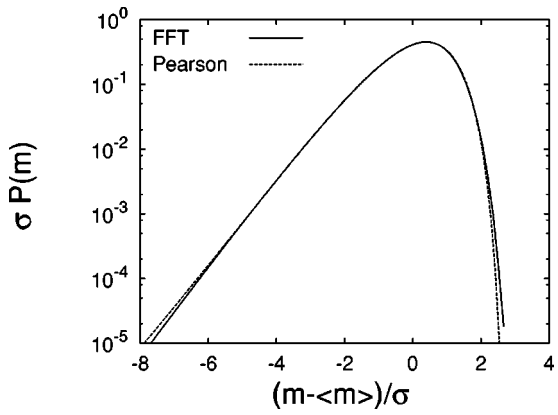

FIG. 8. The PDF compared with the fit obtained with the Pearson method described in the text.

D. Pearson's curve

Pearson [48,49] described an ingenious method of deriving a functional form for a PDF to fit experimental data, given the first four moments of the latter. He considered the differential equation

$$\frac{d\ln y}{dx}=-\frac{x+b}{b_0+b_1x+bx^2} \tag{58}$$

and showed that if y is a distribution, then the parameters b,b_0,b_1 are specific functions of the first four moments. The expression can then be integrated to give (within a normalization factor) an approximate functional form for the PDF, which by definition has the same principal moments as the data to be fitted. The success of Pearson's approach relies on the observation that PDFs with the same moments are approximately coincident over the range of a few standard deviations, which is exactly the range of experimental interest. In the present case, the mean is zero and the standard deviation is set to unity, so the shape of the curve depends only on the skewness, γ, and kurtosis, κ.

We find $\gamma=g_3(2/g_2)^{3/2}=-0.8907$ and $\kappa=3+3g_4(2/g_2)^2=4.415$, which gives the following solution:

$$y=y_0\frac{(\beta-\xi)^q}{(\alpha-\xi)^p} \tag{59}$$

in which $\xi=x-0.397\,23$, $\beta=2.4787$, $\alpha=11.430$, $q=10.249$, $p=47.267$, and $y_0=\exp(105.02)$. Equating $y(x)=\Pi(\theta)$, the fit to the exact expression (Fig. 8) is good between $x=-6$ and $x=2$, but the very large numbers involved in Eq. (59) suggest that this functional form has no physical significance. From this analysis we can conclude that data collapse observed in Ref. [21] should be interpreted as meaning that the third and fourth moments scale with σ and L in the same way as they do in the critical 2D *XY* model.

IV. DISTRIBUTION IN THE *D*-DIMENSIONAL GAUSSIAN MODEL

In this section, we study the asymptotics of the distribution function in general dimension D. It is straightforward to

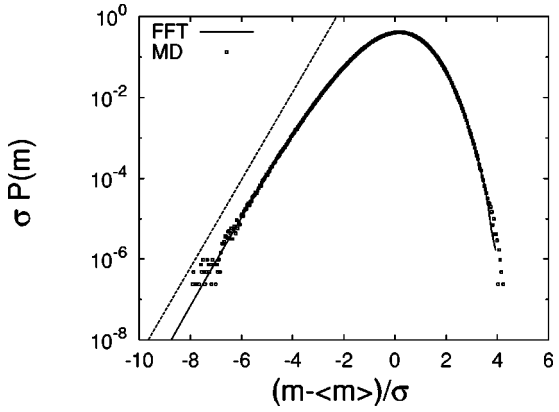

FIG. 9. The PDF in three dimensions for $N=8^3$ and $T/J=1.82$. The dashed line (with slope $\simeq 2.5$) is the exponential asymptote given by Eq. (75) and is shifted with respect to the main curve for clarity.

generalize the development from Eq. (20) to Eq. (22) for arbitrary dimension by redefining $G(\mathbf{q})$ for dimension D and summing over a D-dimensional Brillouin zone. The generalized expression (22) can then be numerically transformed to give $\Pi(\theta)$. The results for $D=3$ and $D=1$ are shown in Figs. 9 and 10, where they are compared with data from Monte Carlo and molecular-dynamics simulations. There is again excellent agreement showing that Eq. (22) is essentially exact in the low-temperature regime, where the Hamiltonian (7) is valid. At higher temperatures, the full Hamiltonian (5) generates vortex structures, Eq. (13) is no longer valid, and the derivation of Eq. (22) breaks down. Within the low-temperature approximation, there are three regimes: $D<2$, $2<D<4$, and $D\geqslant 4$, in addition to the special case $D=2$. The different regimes can be seen from a dimensional analysis of g_1 and g_2. As deviation from Gaussian behavior is due to the abnormal influence of the integral scale in the form of infrared divergences, we can replace G by $1/q^2$ and recalculate the g_k by performing integrals over the Brillouin zone between $2\pi/N^{1/D}$ and 2π. This procedure gives the correct qualitative behavior, but there is a difference between

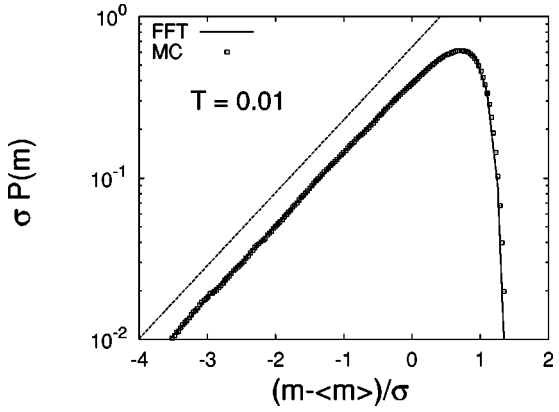

FIG. 10. The PDF in one dimension ($N=128$) at temperature $T/J<12/N$. The dashed line (with slope $\simeq 1.04$) is the exponential asymptote for the low-temperature approximation given by Eq. (65) and is shifted with respect to the main curve for clarity.

the discrete sums and the integrals over the Brillouin zone, even in the thermodynamic limit (see Appendix C). The correct qualitative behavior is

$$g_1 \simeq \begin{cases} C_{1,D} N^{(2-D)/D}, & D<2 \\ A_1 \ln N + B_1, & D=2 \\ C_{1,D}, & D>2 \end{cases} \tag{60}$$

and

$$g_2 \simeq \begin{cases} C_{2,D} N^{2(2-D)/D}, & D<4 \\ (A_2 \ln N + B_2)/N, & D=4 \\ C_{2,D}/N, & D>4. \end{cases} \tag{61}$$

The lower and upper critical dimensions, $D=2$ and $D=4$, are marked by the logarithmic divergence of g_1 and g_2, respectively.

Using the linearized order parameter (24), we find for $D<2$ that g_1 diverges as a power of N giving $\langle m\rangle = 1 - \tau C_{1,D} N^{(2-D)/D}$, which is a poor approximation for a thermodynamic quantity bounded on the interval [0,1]. Once outside this restricted low-temperature region, $\tau \leqslant 1/[C_{1,D} N^{(2-D)/D}]$, both the linear approximation for the order parameter and the quadratic approximation for the Hamiltonian break down and there is a divergence in the behavior of the PDF, as calculated from Eq. (22) and as simulated numerically. The system is, of course, disordered at all temperatures, so that the correct $\langle m\rangle$ and σ both vary as $1/\sqrt{N}$ and the PDF for the vector order parameter is a two-dimensional Gaussian function centered on $\mathbf{m}=0$. The PDF for m, as defined in Eq. (6), is $P(m) \sim m \exp(-m^2/2\sigma^2)$, analogous to a Maxwellian distribution of molecular speeds, and the thermodynamic system satisfies the central-limit theorem (see Appendix A). Results of numerical simulation are shown in Fig. 11. As we have already seen, for $D=2$ the situation is different, as there is a large region of temperature where the quadratic Hamiltonian correctly describes the physics even though Eq. (24) is not a good approximation. In this regime of temperature, the PDFs $\Pi(\theta)$, for parameters (24) and (6) are, however, identical.

For dimension $D>2$, the low-temperature expansion for the order parameter gives consistent results for all N, as long-range order is stable and $\langle m\rangle \sim 1 - C_{1,D}\tau$ is well defined. Above $D=4$, our results agree with mean-field theory ($D=\infty$) where all sites are connected. Here, $\langle m\rangle \simeq 1-\tau/4$ and $\sigma \simeq \tau/2\sqrt{2N}$, and for large but finite N, the universal function Π is simply a Gaussian,

$$\Pi(\theta) = \frac{1}{\sqrt{2\pi}} \exp(-\tfrac{1}{2}\theta^2), \tag{62}$$

which corresponds to the central-limit theorem for a collection of N independent oscillators, each of expectation value $\langle m\rangle$ and standard deviation $\tau/2\sqrt{2N}$.

A. Low-temperature calculation in $D=1$

If the low-temperature calculation for $D<2$ is not terribly pertinent for the thermodynamic system, it highly relevant for the interface problem in the context of the EW model [24,28,29] and is exactly solvable in $D=1$ [28]. In this case, computing the different g_k, we find

$$g_1=N/12, \quad g_2=N^2/720, \ldots, \quad g_p=\frac{2\zeta(2p)}{(2\pi)^{2p}}N^p, \quad p\gg 1,$$

where $\zeta(k)=\Sigma_{i=1}^{\infty} i^{-k}$ is the Riemann zeta function [65]. The expectation value of the magnetization and standard deviation are

$$\langle m\rangle=\exp\left(-\frac{\tau N}{24}\right)\simeq 1-\frac{\tau N}{24},$$

$$\sigma^2=\left(\frac{1}{N}\sum_{\mathbf{r}}\cosh \tau G_R(\mathbf{r})-1\right)\langle m\rangle^2$$

$$=\left(\int_0^1 \cosh \tau N(x^2-x+1/6)dx-1\right)\langle m\rangle^2\sim \tau^2 N^2,$$

which means that the ratio $\langle m\rangle/\sigma$ scales as $1/N$, although for the parameters of the interface problem $\langle w^2\rangle/\sigma_{w^2}\sim O(1)$. We evaluate the universal distribution Π, using the general Eq. (26) with G defined for the $D=1$. After some algebra, we find for $\Pi(\theta)$

$$\Pi(\theta)=\int\frac{dx}{2\pi}\exp\left[ix\left(\theta-\frac{\sqrt{360}}{12}\right)-\sum_{k=1}^{\infty}\ln\left(1-\frac{ix\sqrt{360}}{2\pi^2k^2}\right)\right]$$

$$=\int\frac{dx}{2\pi}\exp\left[ix\left(\theta-\frac{\sqrt{360}}{12}\right)-\ln\left(\frac{\sin\sqrt{ix\sqrt{360}/2}}{\sqrt{ix\sqrt{360}/2}}\right)\right]$$

$$=\int\frac{dx}{2\pi}\exp[i\Phi(x)]. \tag{63}$$

This expression is related directly to the function $\tilde{\Phi}$ of Eq. (11) in Ref. [28]: $\Pi(\theta)=\tilde{\Phi}(2-24\theta/\sqrt{360})$. The method used in [24,28,29] is based on path integration, but the results are the same as our saddle-point method, used to compute the asymptotics. Setting $x=iy$, the extrema of Φ satisfy the equation

$$\theta-\frac{\sqrt{360}}{12}=-\frac{\sqrt{360}}{2\pi^2}\sum_{k=1}^{\infty}\frac{1}{k^2+y\sqrt{360}/2\pi^2}$$

$$=-\frac{\sqrt{360}}{2\pi^2}\left(-\frac{1}{2y\sqrt{360}/2\pi^2}\right.$$

$$\left.+\frac{\pi}{2\sqrt{y\sqrt{360}/2\pi^2}}\coth\pi\sqrt{y\sqrt{360}/2\pi^2}\right). \tag{64}$$

For $\theta\ll -1$, y is close to the first pole $-2\pi^2/\sqrt{360}$ of the right-hand side of Eq. (64), which is similar to the 2D case (30) except that the 1D extrema function is easier to evaluate. Performing the saddle-point computation, we find that Π behaves asymptotically as

$$\Pi(\theta)\propto\exp[2\pi^2\theta/\sqrt{360}], \tag{65}$$

which is the same as [28]. The asymptote (65) is drawn on Fig. 10 where it can be compared with the full calculation and with simulation. The exponential tail is extremely well defined and the predicted slope is clearly correct.

In the regime of fluctuations above the mean, for $y\gg 1$, θ is close to the constant $\sqrt{360}/12$, and no extrema exist for θ beyond this value. In this case, $y\simeq\sqrt{360}/[8(\sqrt{360}/12-\theta)^2]$, and the saddle-point approximation leads to the following asymptotic value for Π near this upper limit:

$$\Pi(\theta)\propto(\sqrt{360}/12-\theta)^{-5/2}\exp(-\tfrac{1}{8}\sqrt{360}/(\sqrt{360}/12-\theta)), \tag{66}$$

which is the same result as [28]. We refer the reader to Refs. [24,28,29] for the precise coefficients in both asymptotic limits.

In conclusion, we find that for $\theta\ll -1$, the universal distribution again has an exponential tail, while for fluctuations above the mean the PDF shoots to zero as $\exp[-3\theta_0/2(\theta-\theta_0)]$, with $\theta_0=\sqrt{360}/12$. This upper limit corresponds to the constraint that $m\leqslant 1$.

It is worth pointing out in some detail here that the exponential tail in the one-dimensional problem is not the result of critical fluctuations. The small deviations in angle $(\theta_i-\theta_j)$ constitute a random walk with $w\sim\sqrt{1-m}$ being the radius of gyration, which scales correctly as the square root of the walk length, L. The 1D linear order parameter or interface problem is therefore nothing more than a simple random walk [28], but despite this the PDF, as shown in Fig. 10, is as follows: a standard result for such a walk is that the mean radius of gyration is proportional to the mean end-to-end distance, S, of the walk. It is easily shown that the PDF $P(S)$ is Gaussian [30]. Changing the variable from S to $X=S^2$, one finds $P(X)\sim X^{-1/2}\exp(-X/X_0)$, a trivial distribution with an exponential tail. The PDF for w^2 has the same exponential tail, but does not show the essential singularity at $w^2=0$ $(m=1)$, thus we conclude that a rather surprising property of a random walk is that the PDFs for the radius of gyration and for the end-to-end distance are not the same. The origin of this difference is that the average angle $\overline{\theta}$, corresponding to the center of mass of an equivalent random walk, fluctuates with L in the same way as the radius of gyration itself, and this lack of self-averaging removes the essential singularity from the PDF at $w^2=0$.

B. Asymptotic solutions in general dimension

We first evaluate the asymptotic value of Π for positive θ by solving the saddle point of Eq. (26), rescaling the variable

$x\sqrt{g_2/2}\to x$ for convenience. For $D<2$, the ratio $g_1/\sqrt{g_2}$ is independent of the system size and, with $x=iy$, the equation to solve is

$$\theta-\frac{g_1}{\sqrt{2g_2}}\propto-\int_{\mathrm{cst}/N^{1/D}}^{\mathrm{cst}}\frac{Nq^{D-1}}{q^2N+y\sqrt{2/g_2}}\,dq, \tag{67}$$

where cst is a constant. By setting $N^{1/D}q/\sqrt{y}\to q$, we find that, for large and positive y,

$$\frac{g_1}{\sqrt{2g_2}}-\theta\propto y^{(D-2)/2}\int_{\mathrm{cst}/\sqrt{y}}^{\mathrm{cst}\,N^{1/D}/\sqrt{y}}\frac{q^{D-1}}{1+q^2}dq$$

$$\sim y^{(D-2)/2}\int_0^\infty\frac{q^{D-1}}{1+q^2}dq, \tag{68}$$

which means that θ is close to the upper bound $g_1/\sqrt{2g_2}$. Replacing the asymptotic value of y for the extrema in the function Φ (26), we find that

$$\ln\Pi(\theta)\sim-\mathrm{cst}\left(\frac{g_1}{\sqrt{2g_2}}-\theta\right)^{D/(D-2)}$$

$$+\text{logarithmic corrections},$$

$$\theta\sim\frac{g_1}{\sqrt{2g_2}},\quad D<2. \tag{69}$$

The logarithmic corrections come partly from the Gaussian integration around the saddle point and partly from other terms in Eq. (68) that are not accurately evaluated within our approximation. Note again that $D=2$ is a special case as, instead of Eq. (68), we have a logarithmic divergence [see Eq. (33)] and subsequently a double exponential fall in Π for large θ. For the interval $2<D<4$, the ratio $g_1/\sqrt{g_2}$ and the integral (68) are no longer finite and so we look to Eq. (30) for the asymptotic behavior:

$$\theta\propto\frac{1}{g_2}\int_{\mathrm{cst}/N^{1/D}}^{\mathrm{cst}}\frac{d^Dq}{Nq^4}\,\frac{y}{1+y\sqrt{2}/(\sqrt{g_2}Nq^2)}. \tag{70}$$

By again setting $N^{1/D}q/\sqrt{y}\to q$ and using the fact that $g_2N^{2(D-2)/D}$ is finite (60), we arrive at

$$\theta\propto y^{(D-2)/2}\int_0^\infty\frac{q^{D-3}dq}{1+q^2},\quad y\gg1. \tag{71}$$

The integral is convergent for $2<D<4$, and by replacing the value for y in the saddle-point approximation, we get the asymptotic form for Π, in the limit of large and positive θ,

$$\ln\Pi(\theta)\sim-\mathrm{cst}\;\theta^{D/(D-2)}+\text{logarithmic corrections},$$

$$\theta\gg1,\quad 2<D<4. \tag{72}$$

In three dimensions, we therefore expect that the logarithm of the distribution falls off like θ^3, well above the mean. We have not tested this in detail, but the PDF does fall off more slowly for $D=3$ than $D=2$, in qualitative agreement with the predictions here. Finally, we note that throughout the range $2<D<4$, the universal PDF is non-Gaussian, but the hyperscaling relation is invalid: $\langle m\rangle/\sigma\sim g_1/\sqrt{g_2}\sim N^{(D-2)/D}$.

For $D>4$, g_2 decreases as $1/N$, consequently Eq. (71) has to be modified. We find, instead of Eq. (71), that

$$\theta\propto y^{(D-2)/2}N^{(4-D)/4}\int_{N^{(D-4)/4D}/\sqrt{y}}^{N^{1/4}/\sqrt{y}}\frac{q^{D-3}dq}{1+q^2}\sim y,\quad N\gg1. \tag{73}$$

We can, in fact, replace the integrand inside the integral by $q^{D-5}dq$ since the integration domain is large, from which we find that the saddle point is proportional to $\theta\gg1$ and deduce that Π is Gaussian on the right-hand side of the curve. The same is true for $D=4$ despite the logarithmic divergence of g_2.

In the opposite limit $\theta\ll-1$, for both $D=1$ and $D=2$ the asymptotic value of the distribution falls down exponentially [Eqs. (32) and (65)]. We would now like to evaluate this limit in general dimensions. In both cases, the coefficient of θ is related to the value of g_2, i.e., $C_{2,D}$. Rewriting Eq. (30) with discrete sums (see also Appendix C), we have

$$\theta=\frac{N^{2(2-D)/D}}{16\pi^4g_2}\sum_{m_i\geqslant0}{}'\frac{1}{(m_1^2+\cdots+m_D^2)}$$

$$\times\frac{y}{(m_1^2+\cdots+m_D^2)+y\sqrt{2/g_2}N^{(2-D)/D}/4\pi^2}, \tag{74}$$

where the sum excludes $m_i=0$, $i=1,\ldots,D$. The saddle-point equation has a solution y that is the pole nearest the origin, $y=-4\pi^2\sqrt{g_2/2}N^{(D-2)/D}$, i.e., for sets of $\{m_i\}$ with one element equal to 1, the others being zero. For $D<4$ and large N, this pole is finite since g_2 compensates $N^{2(D-2)/D}$, so that its value is simply $y=-4\pi^2\sqrt{C_{2,D}/2}$. Applying the saddle-point integration, we find that the dominant term in the logarithm of Π is, below the mean,

$$\ln\Pi(\theta)\sim4\pi^2\sqrt{\frac{C_{2,D}}{2}}\theta,\quad \theta\ll-1,\quad D<4, \tag{75}$$

and is linear in θ for every dimension below 4. Included in Fig. 11 for $D=3$ is a fit, on the left-hand side of the form (75), with $C_{2,3}$ calculated numerically. There is again excellent agreement, which convincingly confirms the presence of the exponential tail. In fact, true exponential behavior is reached for smaller values of θ than for $D=2$.

For $D>4$, the value of this pole diverges like $N^{(D-4)/2D}$, and the previous solution fails. In fact, the solution (73) for positive θ and y is also valid for negative values if $q^{D-1}dq/(q^2+1)$ is replaced by $q^{D-1}dq/(q^2-1)$. Since the integration domain is far from the pole of the denominator, we can approximate the integrand in both cases by $q^{D-5}dq$, and we get the same result as Eq. (73). We therefore finally conclude that Π is also Gaussian on the left-hand side of the curve and the central-limit theorem applies for $D>4$.

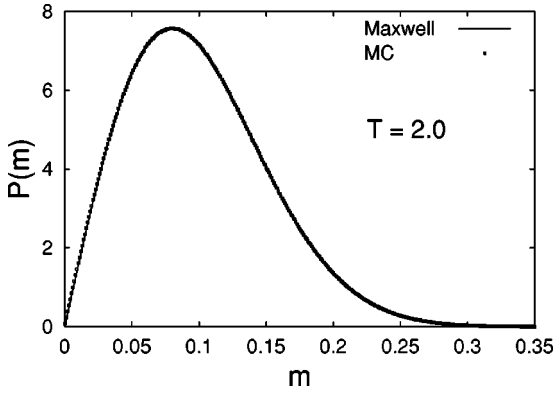

FIG. 11. The PDF in one dimension ($N=128$) at temperature $T/J>12/N$. The continuous line is Maxwell speeds distribution of an ideal gas.

V. CONCLUSION

Probability functions with exponential rather than Gaussian behavior are a common feature of complex systems [33,46,47,53–55]. For example, the PDFs for velocity differences at microscopic scales in fully developed turbulence show exponential tails [53]. This appears to be true in turbulence, not only for microscopic quantities but also for global quantities; the energy injected into a closed turbulent flow being a very well controlled and documented example [10,13,56]. Following these observations, we have proposed that this is also a generic feature of complex systems [11,21]. In this paper we have shown that, for the low-temperature phase of the *XY* model, a critical system at equilibrium, analogous behavior occurs when a few long-wavelength and large-amplitude modes make their presence felt in the global measure, which is typically a sum over $O(N)$ degrees of freedom. The exponential tail can occur in three physically different situations. The first is in two dimensions, when the system is critical and fluctuations occur over all length scales. The second is in one dimension, when the system is not critical, but an exponential tail occurs for a particular global measure, relevant to problems of interface growth, whose moments are completely dominated by the integral scale. The third is in three dimensions, also noncritical, where despite stable long-range order, the large-amplitude long-wavelength modes continue to make their presence felt. The detailed form of the PDF in these three cases is quite different and easily discernible in experiment. In Table I we show the evolution of the skewness and the kurtosis with spatial dimension. The deviations from the Gaussian limit are largest in one dimension, and decrease continually to zero at $D=4$. We propose that the difference in the form of the PDF could be used as an experimental signature of the underlying physics.

TABLE I. Variation of skewness γ and kurtosis κ with dimension D.

D	γ	κ
1	−1.807	8.14
2	−0.891	4.41
3	−0.354	3.31
4	0	3.0

From the general evolution shown in Table I, one might expect a dependence on shape, with dimensional crossover as the length scale in one direction changes from microscopic to macroscopic. This is indeed the case, and for example in two dimensions, the skewness and kurtosis of the PDF calculated from Eq. (22) increase towards the values for $D=1$ if the ratio of lengths in the x and y directions, L_x and L_y, is varied continuously from unity. It would be extremely interesting to establish if the same is true when the length scales are varied in turbulence experiments and numerically in the models of self-organized criticality.

To see how the anisotropy of the PDF comes from the long-wavelength excitations, we give an analysis in reciprocal space: the Hamiltonian (7) is diagonalized,

$$H=\frac{J}{2}\sum_{\mathbf{q}>0} G(\mathbf{q})^{-1}\,\mathrm{Re}\{\phi_{\mathbf{q}}\}^2, \tag{76}$$

where $\phi_{\mathbf{q}}$ is the discrete Fourier transform of θ_i and the sum is over the Brillouin zone [57], with the thermodynamic variable for each $\mathbf{q}$ taken as the real part of $\phi_{\mathbf{q}}$. Defining $m_{\mathbf{q}}=(1/2N)\mathrm{Re}\{\phi_{\mathbf{q}}\}^2$ the linear order parameter can be written $m=1-\Sigma_{\mathbf{q}} m_{\mathbf{q}}$, where the $m_{\mathbf{q}}$ are statistically independent variables with PDF,

$$P(m_{\mathbf{q}})=\sqrt{\frac{\beta J q^2 N}{4\pi}}\,m_{\mathbf{q}}^{-1/2} e^{-\beta J N q^2 m_{\mathbf{q}}}. \tag{77}$$

Here, as we are principally interested in the modes at small $q=|\mathbf{q}|$, we have, without loss of generality, approximated $G(\mathbf{q})^{-1}\approx q^2$. The PDF for m is thus nothing more than the composite PDF for a set of independent spin-wave modes or an ''ideal gas'' of particles, whose only peculiarity is that the mass term varies as q^2. The Goldstone modes have wave vector $q=2\pi/L$ and hence make contributions of $O(1)$ to m, while the modes on the zone edge with $q=\pi$ have only microscopic amplitude. This dispersion in amplitudes is the key to the unusual behavior for $D=2$, as it violates one of the conditions for the central-limit theorem to apply to a sum of statistically independent variables, namely that the individual amplitudes do not differ by too much. However, it is not true that the Goldstone modes, by themselves, give the complete PDF. The mean value $\langle \Sigma_q m_q\rangle \sim \int_{2\pi/L}^{\pi} q^{-2} n(q) dq$, where $n(q)\sim q^{D-1}$ is the density of states. For $D=2$, both limits of the integral are required and a detailed calculation gives $\langle \Sigma_q m_q\rangle=(\eta/4)\ln(CN)$, with $C=1.87$ and with critical exponent $\eta=T/2\pi J$. The anomalous term $\ln N$ therefore reflects the fact that modes from all over the Brillouin zone are relevant for $\langle m\rangle$ and through Eq. (18) for the higher moments $\langle m^p\rangle$.

For $D=1$, only the lower limit of integration is required, the upper limit can be set to ∞, and the constants g_p are proportional to N^p. As a result, the linear development of the order parameter in small angles, Eq. (24), is a very poor approximation for the thermodynamic quantity defined on the interval [0,1]. The two expressions (6) and (24) describe

different physical quantities. The former is directly related to the interface width in the Edwards-Wilkinson model of interface growth. The PDF for the full order parameter is consistent with an uncorrelated system, that is, a paramagnet with a two-dimensional order parameter. For the linear order parameter, the PDF, shown in Fig. 10, does have an exponential tail, but this is not the result of critical fluctuations, rather it is the property of a simple random walk. We remark further that dependence on a macroscopic length scale does not, in itself, indicate critical behavior. Rather, critical behavior is exemplified by the case $D=2$, where all length scales are important between the microscopic and macroscopic cutoff.

$D=3$ represents the opposite of the one-dimensional case: $\langle m \rangle$ is controlled by the upper limit of integration and the result is unchanged by setting the lower limit to zero. However, despite long-range order being stable and the system not being critical in the low-temperature phase, the exponential tail persists. This is related to temperature being a dangerously irrelevant variable [58] near the zero-temperature fixed point of a renormalization-group flow, between the lower and the upper critical dimension. The constant g_2 now falls to zero with system size but it does so more slowly than $1/N$ [see Eq. (61)]. As a result of this slow decay, the ratio $g_p/g_2^{p/2}$, $p>2$ in Eq. (20) is independent of N and the distribution is non-Gaussian, despite g_p and g_2 both being zero in the thermodynamic limit. At low temperature the magnetization is finite, but the Goldstone mode influences the PDF sufficiently to produce an exponential tail. A physical consequence of this anomaly is that the longitudinal susceptibility

$$\chi \sim \frac{N}{T}(\langle m^2 \rangle - \langle m \rangle^2) \sim N^{(4-D)/D} \tag{78}$$

is weakly divergent throughout the ordered phase [14,35]. This is true for all magnetic systems with Heisenberg or XY symmetry. It could therefore be interesting to look for evidence of the departure from Gaussian behavior experimentally in a noncritical three-dimensional system. Precision temperature control would not be required, however as the ratio $\sigma/\langle m \rangle$ falls off as $1/N^{1/3}$, the divergence in the susceptibility is very weak and this phenomenon may be out of experimental reach.

Returning finally to critical systems, we have been able to exploit a system interacting via a quadratic Hamiltonian at exactly the lower critical dimension. In this particular case, one has access to a critical point, with the fluctuation-dominated behavior that this implies, while retaining the benefit of Gaussian integration over phase space. As a result, all critical behavior can be calculated microscopically, without the need for either the renormalization group or the scaling hypothesis. The only price one pays for this simplicity is a critical system with a single independent exponent and the scaling relations satisfied through weak scaling only. In general, we believe that the analytic results that we have obtained are useful for the understanding of finite-size scaling and for the interpretation of experimental observations from more complex correlated systems. The examples we have discussed [11,21] point towards a behavior analogous to criticality for an enclosed turbulent flow and for models showing self-organized criticality. However, the detailed analysis presented here leaves many open questions, and more experiment and simulation are clearly required if the generality and the limits of this proposition are to be tested further.

ACKNOWLEDGMENTS

This work was largely motivated by our collaboration with K. Christensen, H. J. Jensen, S. Lise, J. López, and M. Nicodemi from Imperial College London and we are particularly grateful to H. J. Jensen and M. Nicodemi for bringing the theory of extremal statistics to our attention. In addition, we have greatly benefited from discussions with S. Fauve, N. Goldenfeld, J. Harte, A. Noullez, and Z. Rácz during the SIMU/CECAM planning meeting ''Universal Statistics in Correlated Systems,'' in Lyon, 29–31 March 2000 and from subsequent discussions with L. Berthier, E. Leveque, S. McNamara, P. Pujol, and again Z. Rácz in connection with the 1D problem. It is our pleasure to thank all these people. M.S. is supported by the European Commission (Contract No. ERBFMBICT983561).

APPENDIX A

Some comments on the central-limit theorem in critical systems

The central-limit theorem is a powerful result of probability theory that provides the foundation for statistical thermodynamics [59]. It states that the PDF of the sum $Z=\Sigma_{i=1}^{N} z_i$ of N statistically independent variates z_i tends, in the limit of large N and for moderate values of the variate Z, to a Gaussian distribution. As well as the statistical independence of the z_i, another key criterion for the theorem to hold is that the z_i are *individually negligible* [36,60,61]. At a critical point, the first of these criteria is violated. The 2D XY model is of particular interest here as it is diagonalizable into statistically independent degrees of freedom and maps directly onto a problem where the second criterion is violated: the direct space variables, that is, the spins S_i, are certainly individually negligible for large system size N, but are strongly correlated. On the other hand, when diagonalized in reciprocal space, the spin-wave variables are statistically independent, but are no longer all individually negligible. In particular, the long-wavelength modes make a significant impact on the fluctuations of the global measure, in this case the linearized order parameter (24). The PDF for the full and the linear order parameters are identical, even when the quantities themselves differ, which makes it an ideal system for the practical study of the breakdown of the central-limit theorem. A conventional critical system cannot, in general, be diagonalized in this way, as evidenced by the divergent specific heat.

Strictly speaking, the central-limit theorem does not apply to the compound variate Z, but rather to the normalized quantity $(Z-\langle Z \rangle)/N^{1/2}$. This normalization is essential for a reasonable PDF in the thermodynamic limit, as the standard

deviation for fluctuations about the mean value $\langle Z \rangle$ scales with system size in the same way. If a normalization factor $N^{1/2+\rho}$, $\rho \neq 0$, is chosen, then one obtains a distribution that is concentrated either at zero or infinity [3]. We illustrate this with an example from statistical thermodynamics. The total energy E of an ideal gas of N molecules has a PDF of the form $P(E) \sim E^{3N/2-1} \exp(-\beta E)$. It is straightforward to confirm that $P(E)$ tends to a δ function in the thermodynamic limit, while $P(E/N^{1/2})$ tends to a Gaussian function [62]. One can see from this example that the function is never truly Gaussian, indeed it is always of the form $\ln P \sim (3N/2 - 1)\ln E - \beta E$, which can easily be made independent of N by choosing appropriate units. The central-limit theorem applies because the width of the distribution scales as $N^{1/2}$, which means that fluctuations with any physical significance are all concentrated near the turning point of the function $\ln P$. The theorem only has meaning because of the significance one attaches to values of the variate that differ by only a few standard deviations from the mean. In practical terms, it is therefore essential to normalize fluctuations to the standard deviation in order to test the central-limit theorem.

In the case of dependent variables, the limit distribution can be different from the Gaussian form. Two types of dependent random variables can be defined [3]: (i) weakly dependent, in which the correlation function falls to a constant value in a finite range, and the standard deviation again varies as $\sqrt{N}$; (ii) strongly dependent, in which the fluctuations vary as a power of N different from $\frac{1}{2}$. Case (i) corresponds to a system with a finite correlation length. In case (ii), which includes systems with critical fluctuations, the central-limit theorem does not hold, but a reasonable PDF can be obtained by normalizing to the variance, hence to an appropriate power of N, with $\rho \neq 0$. Defining the (scalar) order parameter to be the intensive quantity $z = Z/N$, and using the scaling relations for a finite system, one finds $\rho = (1 - \eta/2)/D$. The limit distribution is now expected to be non-Gaussian, as can be shown explicitly for the Ising model [4,63]. Note, however, that ρ remains nonzero even at the upper critical dimension (taken as $D = 4$ here) when $\eta = 0$ and where one might legitimately expect a Gaussian PDF. The condition $\rho \neq 0$ may therefore be a necessary but not a sufficient condition to ensure non-Gaussian order-parameter fluctuations.

Case (ii) is not actually limited to critical fluctuations: the example of a dangerously irrelevant variable discussed in the text also falls into this category, with $\rho = 2/D - 1/2$. Here, ρ does go to zero as the upper critical dimension is reached and the danger of the irrelevant temperature variable disappears.

An ordinary critical point is more complicated than those of the 2D XY model. In this case, the correlation length is only infinite precisely at the critical temperature. A non-Gaussian limit function can therefore only be found on a locus of points such that ξ/L is a constant as the thermodynamic limit is taken. Thus, fixing the temperature $T \neq T_C$ and varying N will always cause a transition from non-Gaussian to Gaussian statistics. Conversely, fixing $T = T_C$, one will only arrive at the stable limit function in the thermodynamic limit. One can therefore imagine a set of loci of constant PDF in $[T, L^{-1}]$ space that converge on $[T_C, 0]$. We have suggested [21] that there is one such locus, $[T^*(L), L^{-1}]$, where the PDF has approximately the same form as that of the 2D XY model. Thus, to sit at the critical temperature and change L is not the same as traveling along the locus $[T^*(L), L^{-1}]$. From scaling argument [64] one can check that the tails of the PDF at T_C should have the form $P(m) \sim \exp(-m^{\delta+1})$ in order to yield the correct scaling relation in the presence of a weak magnetic field: $\langle m \rangle \sim h^{1/\delta}$. We do not find this, despite the same scaling relation holding for the 2D XY model with $\delta = 8\pi J/k_B T - 1$. This difference may come from the difference in trajectories in the space of variables T and L.

A final point concerns the central-limit theorem as applied to a vector order parameter, **m**, such as the XY model. In the high-temperature limit, the fluctuations in the vector **m** follow a two-dimensional Gaussian centered on $\mathbf{m} = 0$ and the PDF for the scalar $m = |\mathbf{m}|$ follows a ''Maxwell speed distribution'' for a two-dimensional gas. In an ordered regime and even in the critical regime for $D = 2$ [14], $\sigma \ll \langle m \rangle$, which means m behaves, to an excellent approximation, as a one-dimensional quantity. The symmetry breaking therefore induces a change in topology for the fluctuations in **m**. This is generalizable to order parameters of higher dimension.

APPENDIX B

The graphs g_k can be written, in the large-N limit, in terms of power series. For example,

$$g_2 = \lim_{N\to\infty} \frac{4}{N^2} \sum_{m=1}^{Q} \sum_{n=1}^{Q} \frac{1}{(4 - 2\cos 2\pi m/\sqrt{N} - 2\cos 2\pi n/\sqrt{N})^2} + \frac{4}{N^2} \sum_{m=1}^{Q} \frac{1}{(4 - 2\cos 2\pi m/\sqrt{N})^2}, \tag{B1}$$

where $Q = (\sqrt{N} - 1)/2$. The sum is dominated by the contributions for small m and n, but as the pole $m = 0$, $n = 0$ is explicitly excluded from the sum, it remains finite even in the limit $N \to \infty$. Taking only the first terms in a development of the cosines, which is exact in the thermodynamic limit, one finds

$$g_2=\frac{1}{4\pi^2}\sum_{m=1}^{\infty}\frac{1}{m^4}+\frac{1}{4\pi^4}\sum_{m=1}^{\infty}\sum_{n=1}^{\infty}\frac{1}{(m^2+n^2)^2}$$

$$=\frac{1}{360}+\frac{1}{4\pi^4}\sum_{m=1}^{\infty}\sum_{n=1}^{\infty}\frac{1}{(m^2+n^2)^2}, \tag{B2}$$

and in general, for g_k,

$$g_k=\frac{1}{4\pi^2}\sum_{m=1}^{\infty}\frac{1}{m^{2k}}+\frac{1}{4\pi^4}\sum_{m=1}^{\infty}\sum_{n=1}^{\infty}\frac{1}{(m^2+n^2)^k}. \tag{B3}$$

APPENDIX C

For large and positive y, the functional form of φ is $\varphi(y)\sim(1/8\pi)\ln y+\text{const}$. To evaluate it in detail, we use the results of Appendix B to write

$$\varphi(y)=\lim_{Q\to\infty}\frac{1}{2\pi^2}\sum_{m=1}^{Q}\left(\frac{1}{m^2}-\frac{1}{m^2+\hat{y}}\right)+\frac{1}{2\pi^2}\sum_{m=1}^{Q}\sum_{n=1}^{Q}\left(\frac{1}{m^2+n^2}-\frac{1}{m^2+n^2+\hat{y}}\right), \tag{C1}$$

where $\hat{y}=y/4\pi^2$. The first two summations give, in the limit of large Q, a constant and a function of $\hat{y}$, which tends to zero for large argument:

$$\lim_{y\to\infty}\frac{1}{2\pi^2}\sum_{m=1}^{\infty}\left(\frac{1}{m^2}-\frac{1}{m^2+\hat{y}}\right)=\frac{1}{12}. \tag{C2}$$

The double sum can be rewritten as

$$\frac{1}{2\pi^2}\sum_{m=1}^{Q}\sum_{n=1}^{Q}\left(\frac{1}{m^2+n^2}-\frac{1}{m^2+n^2+\hat{y}}\right)=\frac{1}{2\pi^2}\sum_{m=1}^{Q}\sum_{n=1}^{\infty}\left(\frac{1}{m^2+n^2}-\frac{1}{m^2+n^2+\hat{y}}\right)-R(Q,y), \tag{C3}$$

where R is a correction term that vanishes in the limit of large Q,

$$R(Q,y)=\frac{1}{2\pi^2}\sum_{m=1}^{Q}\sum_{n=Q+1}^{\infty}\left(\frac{1}{m^2+n^2}-\frac{1}{m^2+n^2+\hat{y}}\right). \tag{C4}$$

The sum can be evaluated in the limit $Q\to\infty$ using the Abel-Plana formula [65],

$$\sum_{i=p}^{q}f(i)=\int_p^q f(x)dx+\tfrac{1}{2}f(p)+\tfrac{1}{2}f(q)+2\int_0^{\infty}\frac{\mathrm{Im}[f(q+ix)-f(p+ix)]}{\exp(2\pi x)-1}\,dx, \tag{C5}$$

where f is any real function that satisfied the assumptions in [65]. Applying this to $R(Q,y)$, we have

$$R(Q-1,y)=\frac{1}{2\pi^2}\sum_{m=1}^{Q-1}\frac{1}{m}[\pi/2-\arctan(Q/m)]+\frac{1}{2(m^2+Q^2)}+4Q\int_0^{\infty}\frac{x\,dx}{(x^2-m^2-Q^2)^2+4Q^2x^2}\frac{1}{\exp(2\pi x)-1}$$
$$-\frac{1}{2\pi^2}\sum_{m=1}^{Q-1}\frac{1}{\sqrt{m^2+\hat{y}}}[\pi/2-\arctan(Q/\sqrt{m^2+\hat{y}})]+\frac{1}{2(m^2+\hat{y}+Q^2)}$$
$$+4Q\int_0^{\infty}\frac{x\,dx}{(x^2-m^2-\hat{y}-Q^2)^2+4Q^2x^2}\frac{1}{\exp(2\pi x)-1}.$$

The first term tends, in the large-Q limit, to the integral

$$\sum_{m=1}^{Q-1}\frac{1}{m}[\pi/2-\arctan(Q/m)]\to\int_0^1\frac{dx}{x}[\pi/2-\arctan(1/x)]=-\int_0^1\frac{\ln x\,dx}{1+x^2}=\text{Catalan}. \tag{C6}$$

A similar behavior is found for the fourth term, since in this limit the dependence on $\hat{y}$ of this term vanishes as $\hat{y}/Q^2$. The other terms are corrections proportional to the inverse of some power of Q, so that R vanishes in the large-Q limit. The double sum (C3) can thus be reduced to a simple sum, since

$$\sum_{n=1}^{\infty}\frac{1}{n^2+z^2}=-\frac{1}{2z^2}+\frac{\pi}{2z}\coth\pi z. \tag{C7}$$

We therefore have, for large y,

$$\frac{1}{2\pi^2}\sum_{m=1}^{Q}\sum_{n=1}^{\infty}\left(\frac{1}{m^2+n^2}-\frac{1}{m^2+n^2+\hat{y}}\right)$$
$$=\frac{1}{2\pi^2}\sum_{m=1}^{Q}-\frac{1}{2m^2}+\frac{\pi}{2m}\coth\pi m+\frac{1}{2(m^2+\hat{y})}$$
$$-\frac{\pi}{2\sqrt{m^2+\hat{y}}}\coth\pi\sqrt{m^2+\hat{y}}$$
$$\simeq-\frac{1}{24}+\sum_{m=1}^{\infty}\frac{1}{4\pi\sqrt{m^2+\hat{y}}}(1-\coth\pi\sqrt{m^2+\hat{y}})$$
$$+\frac{1}{4\pi m}(\coth\pi m-1)+\frac{1}{4\pi}\left(\frac{1}{m}-\frac{1}{\sqrt{m^2+\hat{y}}}\right). \tag{C8}$$

The series containing the hyperbolic function of y vanishes in the limit of large y and the asymptotic behavior of the last term can be evaluated with the Abel-Plana formula (C5),

$$\sum_{m=1}^{\infty}\left(\frac{1}{m}-\frac{1}{\sqrt{m^2+\hat{y}}}\right)\simeq\int_1^{\infty}dx\left(\frac{1}{x}-\frac{1}{\sqrt{x^2+\hat{y}}}\right)+\tfrac{1}{2}$$
$$+2\int_0^{\infty}\frac{x\,dx}{(1+x^2)(\exp 2\pi x-1)}$$
$$=\ln(1+\sqrt{1+\hat{y}})-\ln 2+\gamma, \tag{C9}$$

where the constant γ is equal to

$$\gamma=\tfrac{1}{2}+2\int_0^{\infty}\frac{x\,dx}{(1+x^2)(\exp 2\pi x-1)}.$$

This can be proved by again applying the Abel-Plana formula to the function $1/m$, since we know that $\Sigma_{m=1}^{n}1/m \simeq \ln n+\gamma$. The constant $\Sigma_m(1-\coth\pi m)/4\pi m$ in Eq. (C8) can be rewritten as

$$\sum_{m=1}^{\infty}\frac{1}{4\pi m}(\coth\pi m-1)=\sum_{m=1}^{\infty}\frac{1}{2\pi m}\sum_{n=1}^{\infty}\exp(-2\pi mn)$$
$$=-\frac{1}{2\pi}\ln\prod_{n=1}^{\infty}[1-\exp(-2\pi n)], \tag{C10}$$

and finally the results (C8)–(C10) give the asymptotic behavior of φ for large y:

$$\varphi(y)=\frac{1}{8\pi}\ln y+\frac{1}{24}-\frac{1}{4\pi}\ln 4\pi+\frac{\gamma}{4\pi}$$
$$-\frac{1}{2\pi}\ln\prod_{n=1}^{\infty}[1-\exp(-2\pi n)]+\frac{1}{2y}+\cdots. \tag{C11}$$

The last term comes from a further study of the Abel-Plana formula, which gives the other correction terms in the inverse power of y. An identical analysis gives the finite-size magnetization

$$\langle m\rangle=\exp\left(-\frac{\tau}{2}\mathrm{Tr}\,G/N\right), \tag{C12}$$

where $\mathrm{Tr}\,G/N$ can be expanded as

$$\frac{1}{N}\,\mathrm{Tr}\,G=\frac{1}{4\pi}\ln CN$$
$$C=\exp\left\{\frac{\pi}{3}+2\ln\frac{\sqrt{2}}{\pi}+2\gamma-4\ln\prod_{n=1}^{\infty}[1-\exp(-2\pi n)]\right\}$$
$$=1.8456. \tag{C13}$$

[1] A quote attributed to Poincaré, on the ubiquity of the normal distribution, is ''everyone believes in it: experimentalists believing that it is a mathematical theorem, mathematicians believing it is an empirical fact.'' For a critical discussion, see B. de Finetti, *Theory of Probability* (Wiley, New York, 1975).

[2] L. D. Landau and E. M. Lifshitz, *Statistical Physics* (Pergamon, Oxford, 1980), Vol. 1.

[3] M. Cassandro and G. Jona-Lasinio, Adv. Phys. **27**, 913 (1978).

[4] C. Garrod, *Statistical Mechanics and Thermodynamics* (Oxford University Press, Oxford, 1995).

[5] K. G. Wilson and J. Kogut, Phys. Rep. **12**, 75 (1974).

[6] A. D. Bruce, J. Phys. C **14**, 3667 (1981).

[7] K. Binder, Z. Phys. B: Condens. Matter **43**, 119 (1981).

[8] K. Binder, in *Computational Methods in Field Theory*, edited by H. Gauslever and C. B. Lang (Springer-Verlag, Berlin, 1992).

[9] R. Botet and M. Ploszajczak, Phys. Rev. E **62**, 1825 (2000).

[10] R. Labbé, J.-F. Pinton, and S. Fauve, J. Phys. II **6**, 1099 (1996).

[11] S. T. Bramwell, P. C. W. Holdsworth, and J.-F. Pinton, Nature (London) **396**, 552 (1998).

[12] J.-F. Pinton, P. C. W. Holdsworth, R. Labbé, S. T. Bramwell, and J.-Y. Fortin, *Advances in Turbulence VIII*, edited by C. Dopazo *et al.* (CIMNE, Barcelona, 2000).

[13] J-F. Pinton, P. C. W. Holdsworth, and R. Labbé, Phys. Rev. E **60**, R2452 (1999).

[14] P. Archambault, S. T. Bramwell, and P. C. W. Holdsworth, J. Phys. A **30**, 8363 (1997).

[15] P. Archambault, S. T. Bramwell, J.-Y. Fortin, P. C. W. Holdsworth, S. Peysson, and J.-F. Pinton, J. Appl. Phys. **83**, 7234 (1998).

[16] V. L. Berezinskii, Zh. Éksp. Teor. Fiz. **59**, 907 (1970) [Sov. Phys. JETP **32**, 493 (1971)].

[17] J. M. Kosterlitz and D. J. Thouless, J. Phys. C **6**, 1181 (1973).

[18] J. M. Kosterlitz, J. Phys. C **7**, 1046 (1974).
[19] J. Villain, J. Phys. (Paris) **38**, 581 (1975).
[20] J. V. José, L. P. Kadanoff, S. Kirkpatrick, and D. R. Nelson, Phys. Rev. B **16**, 1217 (1977).
[21] S. T. Bramwell, K. Christensen, J.-Y. Fortin, P. C. W. Holdsworth, H. J. Jensen, S. Lise, J. López, M. Nicodemi, J.-F. Pinton, and M. Sellitto, Phys. Rev. Lett. **84**, 3744 (2000).
[22] J. J. Binney, N. J. Dowrick, A. J. Fisher, and M. E. J. Newman, *The Theory of Critical Phenomena* (Clarendon, Oxford, 1992).
[23] J. L. Cardy, *Scaling and Renormalization Group* (Cambridge University Press, Cambridge, 1996).
[24] Z. Rácz and M. Plischke, Phys. Rev. E **50**, 3530 (1994).
[25] N. D. Mermin, Phys. Rev. **176**, 250 (1968).
[26] J. Tobochnik and G. V. Chester, Phys. Rev. B **20**, 3761 (1979).
[27] S. F. Edwards and D. R. Wilkinson, Proc. R. Soc. London, Ser. A **381**, 17 (1982).
[28] G. Foltin, K. Oerding, Z. Rácz, R. L. Workman, and R. K. P. Zia, Phys. Rev. E **50**, 639 (1994).
[29] M. Plischke, Z. Rácz, and R. K. P. Zia, Phys. Rev. E **50**, 3589 (1994).
[30] M. Doi and S. F. Edwards, *The Theory of Polymer Dynamics* (Clarendon, Oxford, 1987).
[31] A. Pimpinelli and J. Villain, *Physics of Crystal Growth* (Cambridge University Press, Cambridge, 1999).
[32] E. J. Gumbel, *Statistics of Extremes* (Columbia University Press, New York, 1958).
[33] J.-P. Bouchaud and M. Mézard, J. Phys. A **30**, 7997 (1997).
[34] S. C. Chapman, G. Rowlands, and N. W. Watkins, e-print cond-mat/0007275.
[35] See, for example, T. Holstein and H. Primakoff, Phys. Rev. **58**, 1098 (1940); V. G. Vaks, A. I. Larkin, and S. A. Pikin, Zh. Éksp. Teor. Fiz. **53**, 1089 (1967) [Sov. Phys. JETP **26**, 647 (1968)]; J. L. Lebowitz and O. Penrose, Phys. Rev. Lett. **35**, 549 (1975); G. F. Mazenko, Phys. Rev. B **14**, 3933 (1976); P. W. Mitchell, R. A. Cowley, and R. Pynn, J. Phys. C **17**, L875 (1984).
[36] W. Feller, *An Introduction to Probability Theory and Its Applications* (Wiley, New York, 1971).
[37] The constant C is often quoted in the literature with a value $C=2$ [20,26,14]. The more precise calculation here (Appendix C) leads to the value $C=1.8456$.
[38] In the context of intermittency in turbulence, this feature has led to analytical calculation of anomalous exponents. See K. Gawedzki and A. Kupiainen, Phys. Rev. Lett. **75**, 3834 (1995); A. Pumir, Europhys. Lett. **34**, 25 (1996); M. Vergassola, Phys. Rev. E **53**, R3021 (1996).
[39] S. Peysson (unpublished).
[40] K. Bury, *Statistical Distributions in Engineering* (Cambridge University Press, Cambridge, 1999).
[41] X. Leoncini, A. D. Verga, and S. Ruffo, Phys. Rev. E **57**, 6377 (1998).
[42] H. Weber and H. J. Jensen, Phys. Rev. B **44**, 454 (1991).
[43] M. Sellitto and P. C. W. Holdsworth (unpublished).
[44] W. H. Press, S. A. Teukolsky, W. T. Vetterling, and B. P. Flannery, *Numerical Recipes* (Cambridge University Press, Cambridge, 1997).
[45] G. Palma, T. Mayer, and R. Labbé, e-print cond-mat/0007289.
[46] B. Derrida and C. Appert, J. Stat. Phys. **94**, 1 (1999).
[47] M. Prähofer and H. Spohn, Physica A **279**, 342 (2000).
[48] K. Pearson, Philos. Trans. R. Soc. London, Ser. A **186**, 343 (1892); **216**, 429 (1916).
[49] W. M. Smart, *Combination of Observations* (Cambridge University Press, Cambridge, 1958).
[50] We note that we have made a similar change of variables for some of the data shown in Ref. [21] in order to have the exponential tail systematically on the left-hand side of the figure. The SOC data for the forest fire, Bak-Tang-Wiesenfeld and Sneppen models, and the correlated extremal data are treated this way.
[51] This analysis gives the mathematical basis for ''fitting an elephant'' with four parameters.
[52] B. Portelli and P. C. W. Holdsworth (unpublished).
[53] U. Frisch, *Turbulence* (Cambridge University Press, Cambridge, 1995).
[54] N. Goldenfeld and L. P. Kadanoff, Science **284**, 87 (1999).
[55] J. Harte, A. Kinzig, and J. Green, Science **284**, 334 (1999).
[56] S. Aumaite, S. Fauve, and J.-F. Pinton, Eur. Phys. J. B **16**, 563 (2000).
[57] F. Wegner, Z. Phys. **206**, 465 (1967).
[58] N. Goldenfeld, *Lectures on Phase Transitions and the Renormalization Group* (Addison-Wesley, Reading, MA, 1992).
[59] A. I. Khinchin, *Mathematical Foundations of Statistical Mechanics* (Dover, New York, 1949).
[60] G. R. Grimmett and D. R. Stirzaker, *Probability and Random Processes* (Oxford University Press, Oxford, 1992).
[61] R. Von Mises, *Mathematical Theory of Probability and Statistics* (Academic, London, 1964).
[62] G. H. Wannier, *Statistical Physics* (Dover, New York, 1987).
[63] R. S. Ellis, *Entropy, Large Deviations, and Statistical Mechanics* (Springer-Verlag, Berlin, 1985).
[64] J.-P. Bouchaud and A. Georges, Phys. Rep. **195**, 128 (1990).
[65] F. W. Olver, *Asymptotics and Special Functions* (AKP Classics, New York, 1997).
[66] T. Antal and Z. Ráez, Phys. Rev. E **54**, 2256 (1996).